# INVESTIGATION OF THE ATMOSPHERIC REACTIONS OF CHLOROPICRIN

William P. L. Carter, Dongmin Luo and Irina L. Malkina

Revised and Resubmitted to
*Atmospheric Environment*

August 30, 1996

College of Engineering, Center for Environmental Research and Technology
University of California
Riverside, CA 92521

96-AP:029J

## ABSTRACT

An experimental and modeling study was conducted to assess the atmospheric impacts of chloropicrin emissions. Chloropicrin absorption cross-sections were measured in the ~270-390 nm wavelength region, and its overall photodecomposition quantum yield under simulated sunlight conditions was found to be 0.87±0.26. In environmental chamber experiments, chloropicrin significantly enhanced rates of NO oxidation, $O_3$ formation, and consumptions of alkanes and other organic reactants. This is attributed to the formation of Cl atoms and $NO_x$ in its photodecomposition. A previously developed atmospheric chemical mechanism was expanded to include chloropicrin and Cl atom reactions. It gave reasonably good simulations of the chamber experiments. This mechanism predicted that when emitted into polluted urban atmospheres, chloropicrin would have between 0.4 and 1.5 times the ozone impact of the average of emitted VOCs on a mass emitted basis. This value varied depending on environmental conditions and assumptions made concerning the photodecomposition mechanism. The data obtained in this study were inconsistent with a previous study of chloropicrin's photodecomposition in air, probably due to differences in the light sources employed.



*Keywords*

Chloropicrin, UV Absorption Cross Sections, Photochemical Smog, Ozone, Air Quality, Pesticides, Environmental Chambers.


## INTRODUCTION

Chloropicrin ($CCl_3NO_2$) is a pesticide which is extensively used in agriculture as a preplant soil fumigant. Although it is injected at a depth of 15 cm or more below the soil surface, it is sufficiently volatile that under normal applications some is expected to be ultimately emitted into the atmosphere. Therefore, if sufficiently reactive, it may contribute to the formation of tropospheric ozone, a major component of photochemical smog in urban and rural areas. Because ground level ozone formation is a serious air quality problem in many areas, pesticides which contribute to ozone formation may be subject to regulation as Volatile Organic Compound (VOC) ozone precursors. However, available information has been inadequate to assess whether this should be the case for chloropicrin.

Organic compounds can react in the atmosphere either with hydroxyl (OH) radicals, with ozone, with $NO_3$ radicals, or by direct photolysis (Finlayson-Pitts and Pitts, 1986; Seinfeld, 1986; Atkinson,

1990). Although reaction with OH is the primary (and in many cases the only significant) means of atmospheric reaction of most VOCs, and reactions with ozone or $NO_3$ reactions can also be important for certain VOCs under some conditions (Atkinson and Carter, 1984; Atkinson, 1990, 1991), chloropicrin is unusual in that direct photolysis appears to be the only significant atmospheric loss process. The OH radical does not react at a significant rate with fully halogenated compounds (Atkinson, 1989, 1994), and there is no evidence or reasonable expectation for OH radical reaction at the nitro group (Atkinson, 1989, 1994). Based on analogous considerations, reaction with $O_3$ (Atkinson and Carter, 1984; Atkinson, 1994) and $NO_3$ radicals (Atkinson, 1991, 1994) at atmospherically significant rates is also considered unlikely.

Evidence that chloropicrin will photolyze in the atmosphere comes from the study of Moilanen *et al.* (1978), who observed a ~20 day photodecomposition half life when irradiated with sunlamps in the presence of $O_2$. Oxygen was apparently involved in the photooxidation process in their system, since no chloropicrin decomposition was observed the photolysis was carried out in $N_2$. The data were explained by invoking a trioxalone intermediate, with the net process being

$$CCl_3NO_2 + h\nu\ (+ O_2) \rightarrow Cl_2CO + ClNO\ (+ O_2) \quad (1)$$

This mechanism was supported by their observations that ClNO is formed in near unit yields at low reaction times. These observations tend to rule out the alternative photodecomposition process,

$$CCl_3NO_2 + h\nu \rightarrow Cl_3C\cdot + NO_2 \quad (2)$$

which should occur regardless of whether $O_2$ is present, and would not be expected to give rise to ClNO. Under atmospheric conditions, any ClNO formed will rapidly photolyze

$$ClNO + h\nu \rightarrow Cl\cdot + NO \quad (3)$$

with a calculated half life of only ~3-4 minutes for direct overhead sun (Peterson, 1976; Atkinson *et al.*, 1996).

Although these reactions do not contribute to $O_3$ formation directly, the formation of Cl atoms could indirectly cause significant ozone formation. This is because Cl reacts rapidly with other VOCs present, leading to ozone formation, and in most cases generating OH radicals which will further react with VOCs to produce ozone.

However, the data of Moilanen *et al.* (1978) were not adequate to provide quantitative estimates of chloropicrin's atmospheric photolysis rate and reactivity. The absolute light intensity was not specified, and only qualitative information was given concerning the spectral characteristics of the light source, which is not the same as that of sunlight (Crosby and Moilanen, 1974). In addition, quantitative information concerning chloropicrin's UV absorption cross sections and atmospheric photodecomposition quantum yields could not be found in the literature.

This paper describes an experimental and modeling study carried out to assess the atmospheric ozone formation potential of chloropicrin, and to make quantitative estimates of how its ozone formation potential compares with those of other VOCs. This study involved (a) measurement of the absorption cross sections of chloropicrin in the wavelength region which will affect its atmospheric photolysis, (b) conducting environmental chamber experiments to study how the presence of chloropicrin affects ozone and other components of photochemical smog under atmospheric conditions, (c) developing a chemical mechanism for the atmospheric reactions of chloropicrin which is consistent with these measurements, and (d) using this mechanism to estimate how the atmospheric ozone impacts of chloropicrin compares with those of other VOCs.

## EXPERIMENTAL METHODS

### *Absorption Cross Section Measurement*

The absorption cross-sections of chloropicrin vapor were measured using a HP 8452A Diode Array UV-Visible spectrophotometer. This is a single-beam, microprocessor controlled, UV/VIS spectrophotometer with collimating optics. The deuterium lamp light source was turned on at least 10 minutes prior to any measurement. Known pressures of the vapor were prepared in an 11 cm all-glass cell using vacuum techniques and a precision capacitance manometer. The cell was covered with aluminum foil between the time it was filled and the cross-section measurement, which was approximately 30 minutes. Two measurements were carried out using pressure 8.22 and 8.83 torr in the cell, respectively. Photodegradation was checked by leaving the sample in spectrophotometer for over 10 minutes and taking spectrum every 2 minutes. The cross-sections were obtained in computer readable form at wavelengths below 280 nm and up to 500 nm where UV or visible absorption is no longer significant. For comparison with literature data, the same procedure was employed for measuring the spectrum of acetaldehyde.

***Environmental Chamber Experiments***

The environmental chamber experiments involved the irradiation of chloropicrin in the presence of other atmospheric pollutants at ppm or sub-ppm levels in air. The experiments were carried out in two 4'x4'x8' FEP Teflon reaction bags located adjacent to each other at one end of an 8' x 12' room with reflective aluminum paneling on all surfaces. Four 6.5 kW xenon arc lights were mounted on the wall opposite the reaction bags. The reaction bags were interconnected with ports containing fans to exchange the contents of the bags, and separate fans were employed to mix the contents within each chamber. The ports were closed and the fans were turned off during the irradiations. The light intensity was measured by $NO_2$ actinometry using both the quartz tube method of Zafonte *et al.* (1977), modified as discussed by Carter *et al.* (1995a,b), and simultaneous measurements of photostationary state concentrations of NO, $NO_2$, and $O_3$ in otherwise pure air (unpublished results from this laboratory). The results of the actinometry experiments yielded $NO_2$ photolysis rates which declined slowly with time as the lamps aged, with the data being fit by a curve giving $NO_2$ photolysis rates of 0.190 - 0.193 $min^{-1}$ during the period of this study. The spectrum of the xenon arc light source was measured several times during each experiment using a LiCor LI-1800 spectroradiometer. As discussed elsewhere (Carter *et al.*, 1995a,b), this light source gives the closest approximation available of the ground-level solar spectrum for an indoor chamber. The chamber was very similar to the Statewide Air Pollution Research Center's Xenon arc Teflon Chamber (SAPRC XTC) which is described in detail elsewhere (Carter *et al.* 1995a,b).

Ozone was monitored using a UV photometric ozone analyzer, NO and "$NO_y$" species which are converted to NO by a heated catalyst (which included chloropicrin) were monitored using a chemiluminescent NO/$NO_x$ monitor, and organic reactants were measured using gas chromatography with FID detection (GC-FID), as described elsewhere (Carter *et al.*, 1993a; 1995b, 1996). Chloropicrin was monitored using both GC-FID and GC with electron capture detection, although the FID instrument yielded more precise data and was used for the primary measurements. The $Cl_2$ used in some experiments was not monitored, so the amounts initially present were calculated based on the amounts injected, which were measured with a precision manometer in a Pyrex bulb of known volume.

The chambers were flushed with dry air from an AADCO air purification system for 6-9 hours on the night before the experiments. The reactants were injected as described previously (Carter *et al.*, 1995a,b). The chloropicrin used in this study was supplied by Niklor Chemical Co. of Long Beach, CA, and was reported to be 99.9% pure. No measurable impurities were observed by GC. The lights were turned on and allowed to warm up for ~30 minutes prior to the irradiation, which was initiated by lifting a panel between them and the reaction bags. The irradiation typically proceeded for 6 hours. After the

run, the contents of the chambers were emptied (by allowing the bag to collapse) and flushed with purified air. Other reactants were obtained from commercial sources as employed in previous studies (Carter *et al.*, 1995c, and references therein).

## CHEMICAL MECHANISMS AND MODELING METHODS

### *General Atmospheric Photooxidation Mechanism*

The starting point for the mechanism in this work was the detailed SAPRC mechanism which is described in detail by Carter (1990), updated as described elsewhere (Carter *et al.*, 1993a; Carter, 1995, Carter *et al., 1996*). This explicitly represents the initial reactions of a large number of different types of organic compounds, but uses a condensed representation for most of their reactive products. The Carter (1990) mechanism was updated to account for new kinetic and mechanistic information for certain classes of compounds as described by Carter et. al. (1993a) and Carter (1995). In addition, modifications were made to the aromatic mechanisms to improve model simulations of experiments carried out using the chamber and light source employed in this study. The previous mechanism tended to underpredict the rates of NO oxidation and $O_3$ formation in the aromatic - $NO_x$ and mixture - $NO_x$ experiments carried out in a chamber using the light source employed in this study (Carter *et al.*, 1995a). However, by adjusting the yields of the two species used to represent aromatic fragmentation products (MGLY and AFG2), and by reducing the AFG2 photolysis rate, this problem was corrected without adversely affecting simulations of experiments in other chambers (unpublished results from this laboratory). A complete listing of the updated general atmospheric photooxidation mechanism used in this study is given elsewhere (Carter *et al.*, 1996).

### *Chloropicrin Photooxidation Mechanism*

Table 1 gives a listing of the reactions which were added to the general mechanism to represent the reactions of chloropicrin and of the chlorine-containing radicals and intermediates which it forms. Footnotes to the table document the sources of the mechanisms and rate constants assumed. As discussed above, the only significant atmospheric loss process for chloropicrin is believed to be photolysis, and in particular it is assumed not to react with OH radicals or Cl atoms to any significant extent. The absorption cross-sections and quantum yields for the photodecomposition were determined as part of this study, as discussed below. Although the data of Moilanen et. al. (1978) indicate that in air the dominant process was formation of $Cl_2CO$ + ClNO (reaction 1), for evaluation purposes we also considered the effect of assuming that the alternative photodecomposition pathway, formation of $CCl_3\cdot$ + $NO_2$ (reaction

2), was the dominant process. These alternatives are referred to as "Model 1" and "Model 2", respectively, in the subsequent discussion.

Phosgene is assumed to be inert under the conditions of these experiments and its subsequent reactions are ignored. However, the ClNO is rapidly photolyzed to NO and chlorine atoms, with the latter undergoing a variety of reactions as discussed in the following section. Reaction 2 also results in the ultimate formation of phosgene and Cl atoms, following the addition of $O_2$ to $CCl_3\cdot$ to form $CCl_3O_2\cdot$, which in the presence of $NO_x$ primarily reacts with NO to form $NO_2$ and $CCl_3O\cdot$. The latter subsequently decomposes to form phosgene and Cl. (The reaction of $CCl_3$ with $NO_2$ to form $CCl_3OONO_2$ has no significant net effect because the reaction is rapidly reversed by decomposition at ambient temperatures. The reactions of $CCl_3O_2\cdot$ with $HO_2$, $RO_2$, and $RCO_3$ are only important once most of the $NO_x$ has been consumed and ozone formation is no longer significant.) The main effective difference between the two models is that Model 2 involves the ultimate formation of $NO_2$ rather than NO, and also converts an additional molecule of NO to $NO_2$ in the process. Because ozone formation in the lower atmosphere is a result of NO to $NO_2$ conversions (Finlayson-Pitts and Pitts, 1986; Seinfeld, 1986; Carter and Atkinson, 1989), this means that Model 2 would predict higher ozone yields than would Model 1.

***$ClO_x$ Reactions***

Prior to this study, the general mechanism did not include provisions for representing compounds such as chloropicrin whose photooxidations introduce chlorine atoms into the system. The reactions which were added to the mechanism to account for the presence of Cl are included in Table 1, and footnotes to Table 1 indicate the sources of the rate constants and mechanisms assumed. Most of the inorganic reactions and reactions of Cl with the simpler organics were taken from the most recent NASA (1994) or IUPAC (Atkinson *et al.*, 1996) evaluations, and are considered to be reasonably well characterized. In addition, except for chloropicrin, all the absorption cross-sections were taken from the IUPAC (Atkinson *et al.*, 1996) tabulations. Some reactions expected or calculated to be of negligible importance in these systems (such as ClO + ClO or $ClO_2$ reactions) have been omitted to simplify the mechanism. (However, we have not carried out a complete sensitivity study, and it is possible that some reactions included in Table 1 could also be neglected.) The greatest uncertainty concerns the reactions of Cl with some of the higher organics, whose mechanisms and (in some cases) rate constants have not been studied. A rate constant of $1 \times 10^{-10}$ $cm^3$ $molec^{-1}$ $s^{-1}$ is used for organics whose Cl rate constants are unknown, and if the products are unknown they are assumed to be the same as those formed in the corresponding OH reaction, except that HCl is also formed. These assumptions present a source of uncertainty in the model simulations of the reactions of chloropicrin in the presence of mixtures containing these compounds.

***Environmental Chamber Simulations***

The ability of the chemical mechanisms to appropriately simulate the atmospheric impacts of chloropicrin's reactions was evaluated by conducting model simulations of the environmental chamber experiments from this study. This required including in the model appropriate representations of chamber-dependent effects such as wall reactions and characteristics of the light source. The methods used are based on those discussed in detail by Carter and Lurmann (1990, 1991), updated as discussed by Carter *et al.* (1993a) and Carter (1995). The photolysis rates were derived from results of $NO_2$ actinometry experiments and direct measurements of the spectra of the light source, similar to the methods used for a comparable chamber as described by Carter *et al.* (1995a,b). The thermal rate constants were calculated using the temperatures measured during the experiments, with the small variations of temperature with time during the experiment being taken into account. The computer programs and modeling methods employed are discussed in more detail elsewhere (Carter *et al.*, 1995b). The specific reactions and parameter values used in the chamber model simulations for this report are given elsewhere (Carter *et al*, 1996).

***Atmospheric Reactivity Simulations***

To estimate its effects on ozone formation under conditions more representative of polluted urban atmospheres, incremental reactivities, defined as the change in $O_3$ caused by adding small amounts of a compound to the emissions, were calculated for chloropicrin for various simulated atmospheric pollution scenarios. Carter (1994) used a series of single-day EKMA box model scenarios (EPA, 1984), derived by the EPA to represent 39 different urban ozone exceedence areas around the United States (Baugues, 1990), to develop various reactivity scales to quantify impacts of VOCs on ozone formation in various environments. It was found that the $NO_x$ levels were the most important factors affecting differences in ozone impacts among VOCs, and that the ranges of relative reactivities in the various scales can be reasonably well represented by three "averaged conditions" scenarios representing three different $NO_x$ conditions. These scenarios were derived by averaging the inputs to the 39 EPA scenarios, with adjustments to the $NO_x$ inputs. In the "maximum reactivity" scenario, the $NO_x$ inputs were adjusted such that the final $O_3$ level is most sensitive to changes in VOC emissions; in the "maximum ozone" scenario the $NO_x$ inputs were adjusted to yield the highest maximum $O_3$ concentration; and in the "equal benefit" scenario the $NO_x$ inputs were adjusted such that relative changes in VOC and $NO_x$ emissions had equal effect on ozone formation. As discussed by Carter (1994), these represent respectively the high, medium and low ranges of $NO_x$ conditions which are of relevance when assessing VOC control strategies for reducing ozone.

The chemical mechanisms used for these atmospheric simulations were the same as those used to simulate the chamber experiments, except that they included reactions for the full variety of emitted VOCs (Carter, 1994), and the portion representing chamber wall effects (Carter and Lurmann, 1990, 1991) was removed. A complete listing of the mechanism is given elsewhere (Carter *et al.*, 1996).

## RESULTS AND DISCUSSION

### *Absorption Cross-Section Measurements*

Absorption cross sections measurements were obtained for chloropicrin in the 190 - 800 nm range, though no sigificant absorption was observed at $\lambda$ > ~370 nm. Two absorption maxima were observed in this region, the first was 1.8±0.1 x $10^{-18}$ $cm^2$ (base e) at 216-220 nm, and the second was 1.73x$10^{-19}$ $cm^2$ at 274-276 nm. The two measurements agreed within ~10% up ~300 nm, but had uncertainties of ~30% in the 300-330 nm absorption tail because of baseline uncertainties. No evidence for photodegradation of chloropicrin was observed during 10 minutes period of spectral measurement in the spectrophotometer. The intensity of absorption at the higher wavelength maximum is in reasonable agreement with the 2.0x$10^{-19}$ maximum at 278.5 nm reported by Haszeldine (1953) for chloropicrin in petroleum ether solution.

The absorption cross-sections measured for chloropicrin and acetaldehyde in the wavelength region of relevance for the lower atmosphere are shown in Figure 1. Shown also in Figure 1 is the spectrum of sunlight for a zenith angle of 60° as given by Peterson (1976), and the spectrum of the xenon arc light source used in our chambers, both given in arbitrary units normalized to yield the same $NO_2$ photolysis rate. Although the ~275 nm absorption maximum for chloropicrin is at a much lower wavelength region than that reaching the lower atmosphere, Figure 1 shows the overlap between chloropicrin's absorption and the solar and chamber light spectrum in the ~300-360 nm region. This indicates that chloropicrin could undergo photodissociation if the quantum yields were sufficiently high. Figure 1 also indicates that the ratio of chloropicrin to $NO_2$ photolysis rates might be expected to be somewhat lower in our chamber than in the atmosphere, though not to such a large extent that the conditions of our experiments can be considered to be unrepresentative of the range of atmospheric conditions.

Figure 1 also shows the difference between the acetaldehyde absorption cross-sections measured in this work and those recommended for use in atmospheric models (Atkinson *et al.*, 1996). The good agreement supports the reliability of our chloropicrin measurements.

***Photolysis Rate Measurements and Atmospheric Lifetime Estimates***

Since photodecomposition is believed to be the only important loss for chloropicrin under the conditions of our experiments, any measured change in chloropicrin concentration during the experiments should be due only to photolysis or dilution. Under these assumptions, the concentration of chloropicrin at time t in the experiment is given by

$$[\text{chloropicrin}]_t = [\text{chloropicrin}]_0 \times \exp[-(k_{phot} + d)t],$$

where $k_{phot}$ and d are the photolysis and dilution rates, respectively. Thus, plots of $\ln([\text{chloropicrin}]_0/[\text{chloropicrin}]_t)$ against time should be straight lines with slopes of $k_{phot}+d$. Figure 2 shows plots of such data for all the chamber experiments containing chloropicrin, where for each experiment the $[\text{chloropicrin}]_0$ value was derived to minimize the intercept, and thus place the data for all the different runs on the same basis. The figure shows that the chloropicrin data in all the experiments are well fit by a straight line with a slope of $(6.4\pm0.2)\times10^{-4}$ $min^{-1}$. The dilution rates in these experiments are estimated to be $(1.1\pm0.5)\times10^{-5}$ $min^{-1}$, as derived from rates of CO decay in a CO - $NO_x$ - air irradiation, or from rates of n-butane decay in separate n-butane - $NO_x$ - air experiments, with the loss of n-butane due to reaction with OH radicals being corrected for using OH radical concentrations estimated from rates of propene decay in the absence of $O_3$ (see Carter *et al.*, 1995b for a discussion of derivation of dilution rates in our environmental chamber experiments.) This yields a chloropicrin photolysis rate of $(6.3\pm0.2)\times10^{-4}$ $min^{-1}$ in our experiments, which corresponds to a half life of ~18 hours. Note that this is much shorter than the ~20 day half life observed in the experiments of Moilanen *et al.* (1978). This indicates that the light source they employed had a significantly lower intensity in the $\lambda < 370$ nm region which affects chloropicrin photolysis.

If unit quantum yields for chloropicrin photodecomposition are assumed, then the calculated chloropicrin photolysis rate in these experiments is $7.2\times10^{-4}$ $min^{-1}$. This is derived from the chloropicrin cross sections measured in this study, together with the measured $NO_2$ photolysis rates and the $NO_2$ absorption cross-sections and quantum yields which are used in the current mechanism (NASA, 1987; Carter, 1990). This has an estimated uncertainty of ~30% because of baseline uncertainties in the absorption cross section measurement. The ratio of the observed photolysis rate to the calculated photolysis rate assuming unit quantum yield thus gives an effective overall photodecomposition quantum yield of 0.87±0.26. Although the uncertainty in this determination does not rule out the possibility of unit photodecomposition quantum yields, for modeling purposes we assume that the overall quantum yield, $\Phi_1+\Phi_2$, is 0.87.

This effective quantum yield is essentially a weighted average of the quantum yields over the entire 300 - 360 nm wavelength region where the chloropicrin absorption overlaps the spectral distribution of the light source. Therefore, it does not provide information on how the actual quantum yields vary with wavelength. However, Figure 1 shows that this overlap region is essentially the same in ground level sunlight as in our chamber, suggesting that it is a reasonable approximation to apply the effective quantum yield derived from the chamber data to atmospheric simulations. If the ground-level actinic fluxes calculated by Peterson (1976) are assumed, then the atmospheric chloropicrin half life is estimated to range from ~3.4 hours for direct overhead sun to ~7.6 hours for a zenith angle of 60 degrees. This means that on clear summer days somewhat more than half of the emitted chloropicrin would be expected to react within one day. The calculated atmospheric half lives is shorter than the ~18 hours in our experiments because of the lower total light intensity in our experiments compared to ambient sunlight, as well as the somewhat lower relative intensity in the 300-350 nm range (see Figure 1). These differences are taken into account in the chamber and atmospheric model calculations discussed below.

***Environmental Chamber Experiments***

Four types of environmental chamber experiments were carried out for this program: (1) characterization and control runs for the purpose of establishing or evaluating chamber conditions for modeling; (2) $Cl_2$ - n-butane runs to evaluate the mechanism's ability to predict the effects of Cl atoms on alkane oxidation and $O_3$ formation independent of uncertainties in chloropicrin's mechanisms; (3) chloropicrin - alkane or chloropicrin - alkane - $NO_x$ - air experiments to evaluate chloropicrin's effects on ozone formation in a chemically simple system; and (4) incremental reactivity experiments, to evaluate the ability of the mechanisms to predict the effect of chloropicrin on ozone in systems more representative of atmospheric pollution episodes. Table 2 gives a summary of the conditions and selected results of a representative n-butane - $NO_x$ control experiment and all the added $Cl_2$ or chloropicrin experiments carried out for this program. Concentration-time plots for selected species in the $Cl_2$ or chloropicrin runs are shown on Figures 3 and 4. The figures also show results of the model simulations of the experiments, using, for the runs containing chloropicrin, both models for its photodecomposition reaction. The results of the various types of experiments are summarized below.

***Control and Characterization Experiments***

Control and characterization experiments were carried out to assure that the model being used to simulate the chloropicrin experiments appropriately represented chamber effects and other experimental conditions (Carter and Lurmann, 1990, 1991, Jeffries *et al.*, 1992, Carter *et al.*, 1995b), and that there were no anomalous conditions which might affect the results. These included actinometry experiments to

measure the light intensity (Zafonte *et al.*, 1977, Carter *et al.*, 1995b), n-butane - $NO_x$ to evaluate the chamber radical source (Carter *et al.*, 1982; Carter *et al.*, 1995a,b) and to serve as controls for comparison with the n-butane - $NO_x$ runs where $Cl_2$ or chloropicrin were added, and propene - $NO_x$, formaldehyde - $NO_x$, surrogate - $NO_x$, and surrogate + formaldehyde - $NO_x$ experiments for comparison with previous data in this chamber. The results of these experiments were consistent with results of previous runs in this and similar chambers (Carter *et al.*, 1995a,b, unpublished results from this laboratory) and with predictions using the model employed in this study. Therefore, the chamber effects will not be discussed in detail here. Experiments where the same mixtures were simultaneously irradiated in each of the two reactors yielded essentially equivalent results.

Table 2 includes the results of a n-butane - $NO_x$ experiment carried out around the time of this study. It is noted that essentially no ozone was formed, and that only a small fraction of the n-butane reacted. This can be compared with the experiments where $Cl_2$ or chloropicrin were added to the n-butane - $NO_x$ irradiation, as discussed below.

***$Cl_2$ - Alkane Experiments***

Two dual-chamber $Cl_2$ - alkane experiments were conducted to assess the ability of the model to predict the effect of Cl formation on alkane oxidation and ozone formation in this system. Both of these runs had equal concentrations of reactants in each of the two simultaneously irradiated reaction chambers, and essentially equivalent results were obtained in each reactor. Run CTC-139 had no added $NO_x$, and as expected no significant ozone formation was observed since $NO_x$ is required for $O_3$ formation. (The small amount of $O_3$ formed could be fit by the model if it was assumed that there was ~1 ppb of NO or $NO_2$ present initially. This is not unreasonable given that offgasing of $NO_x$ is a known wall effect for this type of chamber [Carter and Lurmann, 1990, 1991]). On the other hand, the $Cl_2$ addition caused a significant and rapid consumption of the n-butane present during the first hour of the experiment, which stopped after the initially present $Cl_2$ was apparently consumed. Figure 3 shows that the rate and amount of n-butane consumption was well fit by the model, indicating that the model correctly represents both the amount and photolysis rate of $Cl_2$ in this chamber, as well as the amount of n-butane consumed. The stoichiometry was approximately two molecules of n-butane per molecule of $Cl_2$ added, or one molecule for each Cl atom. The model predicted that all of the n-butane was consumed by reaction with Cl atoms, and consumption by secondarily-formed OH radicals was negligible.

Run CTC-136 was carried out with $NO_x$ present as well as $Cl_2$ and n-butane. Again, the $Cl_2$ caused a significant consumption of n-butane which was reasonably well fit by the model. Although the

model predicted that a non-negligible amount of n-butane was consumed by reaction with OH radicals as well as by reaction with Cl, the amount of n-butane reacted was somewhat less than the absence of $NO_x$, due to the competing reactions of Cl with $NO_x$ and $O_3$. The initial NO oxidation rate was extremely rapid, and significant ozone formation was observed. This can be contrasted with run CTC-135 (Table 2), which had ~3.5 times more n-butane but no added $Cl_2$. The ozone formed and NO oxidized in this experiment is well fit by model predictions (see Figure 3), suggesting that the model may be appropriately representing the $ClO_x$ processes which affect NO oxidation and $O_3$ formation.

***Chloropicrin - Alkane Experiments***

The chloropicrin - alkane and chloropicrin - alkane - $NO_x$ experiments were carried out to determine the effect of chloropicrin on alkane consumption rates in a relatively simple system, and for evaluating the model predictions of these effects. The addition of chloropicrin, like $Cl_2$, significantly enhanced the rate and amount of $O_3$ formed and the amount of alkane consumed. However, much more chloropicrin had to be added than $Cl_2$ to yield a comparable effect, and as shown in Figure 3, the rate of NO consumption and $O_3$ formation was slower. This was because the calculated photolysis rate for chloropicrin in these experiments was over 50 times lower than that for $Cl_2$. Unlike $Cl_2$, the addition of chloropicrin in the absence of $NO_x$ still resulted in significant $O_3$ formation, apparently due to the $NO_x$ produced when chloropicrin photolyzed.

Figure 3 shows that the model gives good simulations of the effect of added chloropicrin on the amounts of alkane reacted regardless of which assumptions are made concerning the chloropicrin photolysis reaction. On the other hand, the calculations using Model 1 (i.e., assuming $\Phi_1 \gg \Phi_2$) consistently underpredicted the amount of ozone formed, while Model 2 (assuming $\Phi_2 \gg \Phi_1$) performed much better in simulating the ozone yields and formation rates, though it might have a slight bias towards overprediction. This is inconsistent with the data of Moilanen *et al.* (1978), which indicate that only Reaction 1 can be significant.

This inconsistency could be due to differences in the light sources employed. The photoreactor employed by Moilanen *et al.* (1978), as described by Crosby and Moilanen (1974), used an "RS Sunlamp" with a borosilicate glass filter. Although the qualitative spectrum they show for that light source indicated significant intensity in the 300-320 nm region, the borosilicate filter may have removed much or all of this, especially if its UV transmission had degraded due to aging. A much lower UV intensity in the $\lambda < 360$ nm region would explain the much longer lifetime observed by Moilanen *et al.* (1978), and provide a rationalization for the significant differences in the apparent reaction mechanisms. It may be

that the trioxalone mechanism proposed by Moilanen *et al.* (1978) (Model 1) is primarily important at the longest wavelength tail of the absorption spectrum, and that the simple C-N scission mechanism (Model 2) may dominate at the shorter wavelengths where most of the photodecomposition is occurring in our system.

***Incremental Reactivity Experiments***

The incremental reactivity experiments consisted of simultaneous irradiation of a "base case" reactive organic gas (ROG) surrogate - $NO_x$ mixture, together with irradiations of the same mixture with chloropicrin added. The ROG - $NO_x$ mixture is designed to be a simplified model of an urban photochemical smog system. Such experiments provide the most direct test of a chemical mechanisms's ability to predict the effect of the compound on ozone formation in the atmosphere (Carter *et al.*, 1993b, 1995c,d). Two types of incremental reactivity experiments were conducted, differing in the base ROG mixtures used to represent the reactive organics in the atmosphere. In the "mini-surrogate" experiments, the base ROG consisted only of n-hexane, ethylene and m-xylene. These are useful because they are directly comparable to an extensive series of similar experiments conducted for other compounds (Carter *et al.*, 1993b, 1995c,d), and because we found such experiments tend to be more sensitive to mechanism differences than experiments using more complex and realistic surrogates (Carter *et al.*, 1995c). In the "full surrogate" experiments, the base ROG is an 8-component mixture of n-butane, n-octane, ethylene, propene, trans-2-butene, toluene, m-xylene, and formaldehyde, whose relative levels were calculated based on analyses of air quality data (Carter *et al.*, 1995c). Calculations indicate that incremental reactivities in such experiments correlate as well with incremental reactivities in the atmosphere as can be obtained with such experiments (Carter *et al.*, 1995c). All these experiments were carried out using the relatively low ROG/$NO_x$ "maximum reactivity" conditions where ozone formation is most sensitive to VOC emissions (Carter, 1994).

The effect of a test compound on NO oxidation and $O_3$ formation in incremental reactivity experiments is assessed by its effect on $\{([O_3]_t-[O_3]_{init})-([NO]_t-[NO]_{init})\}$ (Carter *et al.*, 1993b, 1995c,d, Carter, 1995). As discussed elsewhere (Johnson, 1983; Carter and Atkinson, 1987; Carter and Lurmann, 1991), this gives a direct measure of the amount of conversion of NO to $NO_2$ by peroxy radicals formed in the photooxidation reactions, which is the process directly responsible for ozone formation in the atmosphere, and is useful for assessing reactivity effects under both high-NO and high-$O_3$ conditions. This quantity is referred to as d($O_3$-NO) in the subsequent discussion.

Table 2 summarizes the ozone yields and fractions of m-xylene and the least reactive of the ROG surrogate alkane reacted in the base case and in the chloropicrin reactivity experiments. Figure 4 shows concentration time plots of d($O_3$-NO) and the alkane in these experiments, together with results of model calculations. The open symbols in Figure 4 show the data in the base case experiment without chloropicrin, and the filled symbols show the effect of the chloropicrin addition. Figure 4 also plots experimental vs calculated chloropicrin incremental reactivity, defined as the change in d($O_3$-NO) caused by adding the chloropicrin, divided by the amount added (Carter *et al.*, 1993b, 1995d), for each hour in the experiments.

The results show that chloropicrin addition has a significant effect on ozone formation and ROG reaction rates even at concentrations of ~0.1 ppm. The effect of chloropicrin on $O_3$ and d($O_3$-NO) is somewhat greater in the experiments using the mini-surrogate base ROG than using the full surrogate. This is consistent with results we have observed with other VOCs (Carter *et al.*, 1995c). On the other hand, the effect of adding a given amount of chloropicrin on n-butane consumption appears to be somewhat less dependent on which ROG surrogate is employed. The addition of formaldehyde has about the same effect on d($O_3$-NO) in a full surrogate experiment as does the addition of a comparable amount of chloropicrin (compare run CTC-128 with run CTC-124 on Figure 4). This suggests that these two compounds may have similar ozone impacts on a per-mole basis under these experimental conditions. However, formaldehyde had a much smaller effect than chloropicrin on the amount of n-butane reacted. This is consistent with the formation of Cl atoms being the main reason for the relatively large effect of chloropicrin on alkane consumption rates. The addition of chloropicrin also increases the rate of consumption of the more reactive species such as m-xylene (see Table 2), but the relative effect is smaller because more of these compounds react in any case.

As was the case with the chloropicrin - alkane experiments, the models (see Figure 4) gave good predictions of the effects of chloropicrin on amounts of alkane reacted. However, the ability to predict the effect on ozone formation and NO oxidation depend on which photolysis mechanism is assumed. The results are somewhat ambiguous in this regard, with Model 2 giving a much better fit to the mini-surrogate experiment with the highest amount of added chloropicrin, while Model 1 gave somewhat better fits to the mini-surrogate experiments with the lower amounts added. The model simulations of the full surrogate experiments were inconclusive, with Model 1 tending to slightly underpredict reactivity and model 2 tending to slightly overpredict the measured d($O_3$-NO) reactivities. However, the fits for Model 2 are slightly better. The overall incremental reactivity data tend to be slightly more consistent with Model 2

than Model 1 since the inconsistencies found with Model 2 are usually not far outside the experimental uncertainty, and the discrepancy in the Model 1 simulation of CTC-112 is significant.

***Atmospheric Ozone Impact Estimates***

Table 3 summarizes the relative ozone impacts calculated for chloropicrin and selected other representative compounds for the averaged conditions scenarios representing the three atmospheric $NO_x$ conditions. The tabulated quantities are "relative reactivities" (Carter, 1994), defined as the ratios of calculated incremental reactivities of the compounds, quantified on an ozone per gram basis, divided by the weighed average of the incremental reactivity of all the reactive organic emissions used in the model. Thus if the relative reactivity of a compound is greater than one, controlling emissions of that compound will have a greater impact on $O_3$ reduction in that scenario than controlling emissions of all ROGs equally. Note also that the reactivity relative to ethane has been the major criterion that the EPA has used in determining whether a VOC has a sufficiently low ozone impact that it would consider exempting it from regulation as a VOC ozone precursor (Dimitriades, 1994). For example, acetone has recently been exempted from regulation because its range of reactivity under various atmospheric conditions overlaps that of ethane.

Table 3 shows that regardless of which chloropicrin photodecomposition mechanism is assumed, the model predicts that chloropicrin has a significantly greater ozone impact than ethane, and thus is not a reasonable candidate for VOC exemption by the criterion used by the EPA. Its reactivity relative to the average emissions depends on the $NO_x$ conditions. Under the relatively high $NO_x$ "maximum reactivity" conditions it is about 40-50% as reactive as the average, while under the lower $NO_x$ "equal benefit" conditions it is ~20-50% more reactive than the average, depending on the mechanism assumed. Under maximum reactivity and maximum ozone conditions (which represent the range most relevant to ozone control strategies because ozone is less sensitive to changes of VOC emissions under lower $NO_x$ conditions), the ozone impact of chloropicrin is comparable to or slightly greater than those of the mid-range alkanes, and considerably less than those for the olefins, most aromatics, or formaldehyde.

The greater relative reactivity of chloropicrin under low $NO_x$ conditions is attributed to the fact that the reaction of chloropicrin introduces $NO_x$ into the system, and $O_3$ formation under these conditions is extremely sensitive to $NO_x$ inputs. Under higher $NO_x$ conditions, the reactivity of chloropicrin is influenced primarily by the fact that its photolysis tends to increase the level of radicals in the system, which increases the rate of $O_3$ formation from all the VOCs present (Carter, 1994; Carter and Atkinson, 1989). The reactivities calculated using Model 2 are uniformly higher than those calculated using Model

1 because the latter involves two more NO to $NO_2$ conversions, the process which is ultimately responsible for $O_3$ formation in the overall reaction. However, both models introduce radicals and $NO_x$ into the system, and thus predict the same qualitative dependence of chloropicrin reactivity on environmental conditions.

## CONCLUSIONS

Chloropicrin has been found to be a relatively reactive compound under simulated atmospheric conditions, and, if emitted in the presence of other reactive organic compounds and $NO_x$, it will have a non-negligible effect on tropospheric ozone formation. Although chloropicrin is unlike most reactive organic compounds in that it does not react to a significant extent with hydroxyl radicals, its photodecomposition is relatively rapid, having a calculated atmospheric half life of somewhat less than a day under clear sky summer conditions. Its absorption spectrum overlaps the spectrum of ground level sunlight in the 300 - 360 nm region, and it photolyzes relatively efficiently in this region (with an 87±13% overall quantum yield) to form both $NO_x$ and Cl atoms. The formation of Cl atoms enhances $O_3$ formation because Cl reacts rapidly with other organic species present in the atmosphere. This is particularly true for alkanes, which would otherwise react much more slowly, and whose subsequent reactions cause ozone formation. The formation of Cl atoms also enhance the overall levels of radicals in the system. The formation of $NO_x$ also gives chloropicrin a relatively high $O_3$ impact under low $NO_x$ conditions where $O_3$ yields are highly sensitive to $NO_x$ inputs. On an ozone formed per gram emitted basis, chloropicrin is estimated to have about half to 1.5 times the ozone impact as the average for emitted VOCs, with the relative impact being greater when $NO_x$ levels are low.

The results of this study differ from the previous study of chloropicrin's gas-phase photolysis (Moilanen *et al.*, 1978) in several important respects. The chloropicrin photolytic lifetime reported by Moilanen *et al.* (1978) is at least an order of magnitude longer than we observed. Our environmental chamber data are more consistent with the photodecomposition reaction occurring via simple C-N scission, rather than the $O_2$-dependent processes which Moilanen *et al.* (1978) proposed. The differences may be due to differences in the light sources employed. Uncertainty in the exact chloropicrin photodecomposition mechanism causes us to conclude that there is a ~25-40% uncertainty in the estimates of the atmospheric ozone impact of chloropicrin, which is not sufficient to affect our overall conclusions about its relative ozone impact compared to other VOCs.

## ACKNOWLEDGEMENTS

This work was supported by the Chloropicrin Manufacturers' Task Force. We also acknowledge the National Renewal Energy Laboratory for providing funding for the xenon arc light source which was employed in this study. Additional funding for the chemical mechanism development effort for the $ClO_x$ reactions was provided by the California Air Resources Board through Contract no. 92-329. The authors also thank Dr. Roger Atkinson for many helpful discussions, Mr. Dennis Fitz, Mr. Kurt Bumiller and Ms. Kathalena Smihula for assistance in carrying out the experiments, and members of the Chloropicrin Manufacturers' Task Force for helpful comments when reviewing the manuscript.

## REFERENCES

Atkinson, R. and S. M. Aschmann (1985): Int. J. Chem. Kinet. 17, 33.

Aschmann, S. A. and R. Atkinson (1995): "Rate Constants for the Gas-Phase Reactions of Alkanes with Cl Atmos at 296±2 K," Int. J. Chem. Kinet, 27, 613-622.

Atkinson, R. (1989): "Kinetics and Mechanisms of the Gas-Phase Reactions of the Hydroxyl Radical with Organic Compounds," J. Phys. Chem. Ref. Data, Monograph no 1.

Atkinson, R. (1990): "Gas-Phase Tropospheric Chemistry of Organic Compounds: A Review," Atmos. Environ., 24A, 1-24.

Atkinson, R. (1991a): "Kinetics and Mechanisms of the Gas-Phase Reactions of the $NO_3$ Radical with Organic Compounds," J. Phys. Chem. Ref. Data, 20, 459-507.

Atkinson, R. (1994): "Gas-Phase Tropospheric Chemistry of Organic Compounds," J. Phys. Chem. Ref. Data, Monograph No. 2.

Atkinson, R., D. L. Baulch, R. A. Cox, R. F. Hampson, Jr., J. A. Kerr, M. J. Rossi, and J. Troe (1996): "Evaluated Kinetic, Photochemical and Heterogeneous Data for Atmospheric Chemistry: Supplement V., IUPAC Subcommittee on Gas Kinetic Data Evaluation for Atmospheric Chemistry," J. Phys. Chem. Ref. Data, in press.

Atkinson, R. and W. P. L. Carter (1984): "Kinetics and Mechanisms of the Gas-Phase Reactions of Ozone with Organic Compounds under Atmospheric Conditions," Chem. Rev. 1984, 437-470.

Baugues, K. (1990): "Preliminary Planning Information for Updating the Ozone Regulatory Impact Analysis Version of EKMA," Draft Document, Source Receptor Analysis Branch, Technical Support Division, U. S. Environmental Protection Agency, Research Triangle Park, NC, January.

Carter, W. P. L. (1990): "A Detailed Mechanism for the Gas-Phase Atmospheric Reactions of Organic Compounds," Atm. Environ., 24A, 481-518.

Carter, W. P. L. (1994): "Development of Ozone Reactivity Scales for Volatile Organic Compounds," J. Air and Waste Manage. Assoc., 44, 881-899.

Carter, W. P. L. (1995): "Computer Modeling of Environmental Chamber Measurements of Maximum Incremental Reactivities of Volatile Organic Compounds," Atmos. Environ., 29, 2513-2517.

Carter, W. P. L. and R. Atkinson (1987): "An Experimental Study of Incremental Hydrocarbon Reactivity," Environ. Sci. Technol., 21, 670-679

Carter, W. P. L., R. Atkinson, A. M. Winer, and J. N. Pitts, Jr. (1982): "Experimental Investigation of Chamber-Dependent Radical Sources," Int. J. Chem. Kinet., 14, 1071.

Carter, W. P. L. and R. Atkinson (1989): "A Computer Modeling Study of Incremental Hydrocarbon Reactivity", Environ. Sci. and Technol., 23, 864.

Carter, W. P. L, D. Luo, I. L. Malkina, and J. A. Pierce (1993a): "An Experimental and Modeling Study of the Photochemical Ozone Reactivity of Acetone," Final Report to Chemical Manufacturers Association Contract No. KET-ACE-CRC-2.0. December 10.

Carter, W. P. L., J. A. Pierce, I. L. Malkina, D. Luo and W. D. Long (1993b): "Environmental Chamber Studies of Maximum Incremental Reactivities of Volatile Organic Compounds," Report to Coordinating Research Council, Project No. ME-9, California Air Resources Board Contract No. A032-0692; South Coast Air Quality Management District Contract No. C91323, United States Environmental Protection Agency Cooperative Agreement No. CR-814396-01-0, University Corporation for Atmospheric Research Contract No. 59166, and Dow Corning Corporation. April 1. (This report is available on the Internet by anonymous FTP at cert.ucr.edu, directory pub/carter/pubs.)

Carter, W. P. L., D. Luo, I. L. Malkina, and J. A. Pierce (1995a): "Environmental Chamber Studies of Atmospheric Reactivities of Volatile Organic Compounds. Effects of Varying Chamber and Light Source," Final report to National Renewable Energy Laboratory, Contract XZ-2-12075, Coordinating Research Council, Inc., Project M-9, California Air Resources Board, Contract A032-0692, and South Coast Air Quality Management District, Contract C91323, March 26. (This report is available on the Internet by anonymous FTP at cert.ucr.edu, directory pub/carter/pubs.)

Carter, W. P. L., D. Luo, I. L. Malkina, and D. Fitz (1995b): "The University of California, Riverside Environmental Chamber Data Base for Evaluating Oxidant Mechanism. Indoor Chamber Experiments through 1993," Report submitted to the U. S. Environmental Protection Agency, EPA/AREAL, Research Triangle Park, NC., March 20.. (This report and database are available on the Internet by anonymous FTP at cert.ucr.edu, directories pub/carter/pubs and /pub/carter/chdata.)

Carter, W. P. L., D. Luo, I. L. Malkina, and J. A. Pierce (1995c): "Environmental Chamber Studies of Atmospheric Reactivities of Volatile Organic Compounds. Effects of Varying ROG Surrogate and $NO_x$," Draft final report to Coordinating Research Council, Inc., Project ME-9, California Air

Resources Board, Contract A032-0692, and South Coast Air Quality Management District, Contract C91323. March 24. (This report is available on the Internet by anonymous FTP at cert.ucr.edu, directory pub/carter/pubs.)

Carter, W. P. L., D. Luo, and I. L. Malkina (1996): "Investigation of the Atmospheric Reactions of Chloropicrin," final report to the Chloropicrin Manufacturers' Task Force, Niklor Chemical Co., Long Beach, CA, May, 1996. (This report is available on the Internet by anonymous FTP at cert.ucr.edu, directory pub/carter/pubs.)

Carter, W. P. L., and F. W. Lurmann (1990): "Evaluation of the RADM Gas-Phase Chemical Mechanism," Final Report, EPA-600/3-90-001.

Carter, W. P. L. and F. W. Lurmann (1991): "Evaluation of a Detailed Gas-Phase Atmospheric Reaction Mechanism using Environmental Chamber Data," Atm. Environ. 25A, 2771-2806.

Carter, W. P. L., J. A. Pierce, D. Luo, and I. L. Malkina (1995): "Environmental Chamber Study of Maximum Incremental Reactivities of Volatile Organic Compounds," Atmos. Environ. 29, 2499-2511.

Crosby, D. G. and K. W. Moilanen (1974): "Vapor-Phase Photodecomposition of Aldrin and Dieldrin," Arch. Environ. Contam. Toxicol. 2, 62-74.

Dimitriades, B. (1994): U. S. Environmental Protection Agency, Atmospheric Research and Exposure Assessment Laboratory, Research Triangle Park, NC, personal communication.

EPA (1984): "Guideline for Using the Carbon Bond Mechanism in City-Specific EKMA," EPA-450/4-84-005, February.

Finlayson-Pitts, B. J. and J. N. Pitts, Jr. (1986): "Atmospheric Chemistry: Fundamentals and Experimental Techniques," John Wiley & Sons, New York.

Haszeldine (1953): "Studies in Spectroscopy, Part IV," J. Chem Soc (London), 1953, 2525-2527.

Jeffries, H. E., M. W. Gery and W. P. L. Carter (1992): "Protocol for Evaluating Oxidant Mechanisms for Urban and Regional Models," Report for U. S. Environmental Protection Agency Cooperative Agreement No. 815779, Atmospheric Research and Exposure Assessment Laboratory, Research Triangle Park, NC.

Johnson, G. M. (1983): "Factors Affecting Oxidant Formation in Sydney Air," in "The Urban Atmosphere -- Sydney, a Case Study." Eds. J. N. Carras and G. M. Johnson (CSIRO, Melbourne), pp. 393-408.

NASA (1987): "Chemical Kinetics and Photochemical Data for Use in Stratospheric Modeling. Evaluation Number 8", JPL Publication 87-41, Jet Propulsion Laboratory, Pasadena California, September.

NASA (1994): "Chemical Kinetics and Photochemical Data for Use in Stratospheric Modeling, Evaluation Number 11," JPL Publication 94-26, Jet Propulsion Laboratory, Pasadena, California, December.

Peterson, J. T. (1976): "Calculated Actinic Fluxes (290 - 700 nm) for Air Pollution Photochemistry Applications", EPA-600/4-76-025, June.

Seinfeld, J. H. (1986): "Atmospheric Chemistry and Physics of Air Pollution," John Wiley & Sons, New York.

Wallington, T. J., L. M. Skewes, and W. O. Siegl (1988): J. Photochem. Photobiol. A:Chem, 45, 33.

Moilanen, K. W., D. G. Crosby, J. R. Humphrey, and J. W. Giles (1978): "Vapor-Phase Photodecomposition of Chloropicrin (Trichloronitormethane)," Tetrahedron, 34, 2245-3349.

Zafonte, L., P. L. Rieger, and J. R. Holmes (1977): "Nitrogen Dioxide Photolysis in the Los Angeles Atmosphere," Environ. Sci. Technol. 11, 483-487.

Table 1. Listing of the reactions added to the general atmospheric photooxidation mechanism to represent the atmospheric reactions of chloropicerin amd chlorine containing species. [a]

| Kinetic Parameters [b] | | | | Notes | Reactions [c] |
|---|---|---|---|---|---|
| k(300) | A | Ea | B | [d] | |
| Reactions of Chloropicerin. (Model 1: $\Phi_1$=0.87, $\Phi$2=0; Model 2: $\Phi_1$=0, $\Phi_2$=0.87) | | | | | |
| (See note 1) | | | | 1 | CCL3NO2 + HV = $\Phi_1$ {CLNO + CL2CO} + $\Phi_2$ {CCL3O2. + NO2} |
| 3.19E-22 | (Falloff Kinetics) | | | 2 | CCL3O2. + NO2 = CCL3O2NO2 |
| k0 = | 3.20E-28 | 0.00 | -7.70 | | |
| kINF = | 7.50E-12 | 0.00 | 0.00 | | |
| F= 0.2 | | | | | |
| 9.56E-12 | (Falloff Kinetics) | | | 2 | CCL3O2NO2 = CCL3O2. + NO2 |
| k0 = | 6.30E-03 | 20.34 | 0.00 | | |
| kINF = | 4.80E+16 | 23.49 | 0.00 | | |
| F= 0.2 | | | | | |
| (Same k as for RO2. ) | | | | 2,3 | CCL3O2. + NO = CL. + CL2CO + NO2 |
| (Same k as for RO2. ) | | | | 2,3 | CCL3O2. + HO2. = CCL3OOH + O2 |
| (Same k as for RO2. ) | | | | 2,3 | CCL3O2. + RO2. = 0.5 {CCL3OH + CL2CO + CL.} |
| ClOx Reactions Added to Mechanism | | | | | |
| (Phot. File = CL2 ) | | | | 4 | CL2 + HV = 2 CL. |
| (Phot. File = CLNO ) | | | | 4 | CLNO + HV = CL. + NO |
| 9.05E-32 | (No T Dependence) | | | 5 | CL. + NO + M = CLNO + M |
| 1.30E-24 | (Falloff Kinetics) | | | 5 | CL. + NO2 = CLONO |
| k0 = | 1.30E-30 | 0.00 | -2.00 | | |
| kINF = | 1.00E-10 | 0.00 | -1.00 | | |
| F= 0.6 | | | | | |
| 1.80E-25 | (Falloff Kinetics) | | | 5 | CL. + NO2 = CLNO2 |
| k0 = | 1.80E-31 | 0.00 | -2.00 | | |
| kINF = | 1.00E-10 | 0.00 | -1.00 | | |
| F= 0.6 | | | | | |
| (Phot. File = CLONO ) | | | | 4 | CLONO + HV = CL. + NO2 |
| (Phot. File = CLNO2 ) | | | | 4 | CLNO2 + HV = CL. + NO2 |
| 3.17E-11 | 1.80E-11 | -0.34 | 0.00 | | CL. + HO2. = HCL + O2 |
| 9.15E-12 | 4.10E-11 | 0.89 | 0.00 | | CL. + HO2. = CLO. + HO. |
| 1.22E-11 | 2.90E-11 | 0.52 | 0.00 | | CL. + O3 = CLO. + O2 |
| 2.40E-11 | (No T Dependence) | | | | CL. + NO3 = CLO. + NO2 |
| 1.65E-11 | 6.20E-12 | -0.58 | 0.00 | | CLO. + NO = CL. + NO2 |
| 1.59E-25 | (Falloff Kinetics) | | | | CLO. + NO2 = CLONO2 |
| k0 = | 1.60E-31 | 0.00 | -3.40 | | |
| kINF = | 2.00E-11 | 0.00 | 0.00 | | |
| F= 0.5 | | | | | |
| k = kEQ x k(CLO.+NO2), kEQ = | | | | 6 | CLONO2 = CLO. + NO2 |
| 4.02E+08 | 5.20E+25 | 23.49 | 3.40 | | |
| (Phot. File = CLONO2 ) | | | | 4 | CLONO2 + HV = 0.9 {CL. + NO3} + 0.1 {O + CLONO} |
| 1.16E-11 | 6.80E-12 | -0.32 | 0.00 | | CL. + CLONO2 = CL2 + NO3 |
| 4.90E-12 | 4.60E-13 | -1.41 | 0.00 | | CLO. + HO2. = HOCL + O2 |
| (Phot. File = HOCL ) | | | | 4 | HOCL + HV = HO. + CL. |
| (neglected) | | | | 7 | CLO. + CLO. = products |
| Cl + VOC and Cl + VOC Product Reactions Added to Mechanism | | | | | |
| 1.07E-13 | 9.60E-12 | 2.68 | 0.00 | | CL. + CH4 = HCL + HCHO + RO2-R. + RO2. |
| 5.90E-11 | 8.10E-11 | 0.19 | 0.00 | | CL. + ETHANE = HCL + CCHO + RO2-R. + RO2. |
| 1.94E-10 | (No T Dependence) | | | 8 | CL. + N-C4 = HCL + 0.076 RO2-N. + 0.924 RO2-R. + 0.397 R2O2. + 0.001 HCHO + 0.571 CCHO + 0.14 RCHO + 0.533 MEK + -0.076 -C + 1.397 RO2. |
| 2.99E-10 | (No T Dependence) | | | 8 | CL. + N-C6 = HCL + 0.185 RO2-N. + 0.815 RO2-R. + 0.738 R2O2. + 0.02 CCHO + 0.105 RCHO + 1.134 MEK + 0.186 -C + 1.738 RO2. |
| 4.05E-10 | (No T Dependence) | | | 8 | CL. + N-C8 = HCL + 0.333 RO2-N. + 0.667 RO2-R. + 0.706 R2O2. + 0.002 RCHO + 1.333 MEK + 0.998 -C + 1.706 RO2. |
| 5.82E-11 | (No T Dependence) | | | 9,10 | CL. + TOLUENE = HCL + RO2-R. + BALD + RO2. |
| 1.20E-10 | (No T Dependence) | | | 10,11 | CL. + M-XYLENE = HCL + RO2-R. + BALD + RO2. + -C |
| 1.60E-23 | (Falloff Kinetics) | | | | CL. + ETHENE = RO2-R. + RO2. + HCHO + HCLCO |
| k0 = | 1.60E-29 | 0.00 | -3.50 | | |
| kINF = | 3.00E-10 | 0.00 | 0.00 | | |
| F= 0.6 | | | | | |
| 2.41E-10 | (No T Dependence) | | | 9 | CL. + PROPENE = RO2-R. + RO2. + 0.5 {HCLCO + HCHO + CLCCHO + CCHO} |
| 2.70E-10 | (No T Dependence) | | | 12 | CL. + T-2-BUTE = RO2-R. + RO2. + CCHO + CLCCHO |
| 7.32E-11 | 8.20E-11 | 0.07 | 0.00 | | CL. + HCHO = HCL + HO2. + CO |
| 7.20E-11 | (No T Dependence) | | | | CL. + CCHO = HCL + CCO-O2. + RCO3. |
| 1.20E-10 | (No T Dependence) | | | | CL. + RCHO = HCL + C2CO-O2. + RCO3. |

Table 1 (continued)

| Kinetic Parameters [b] | | | | Notes | Reactions [c] |
|---|---|---|---|---|---|
| k(300) | A | Ea | B | [d] | |
| 3.50E-12 | (No T Dependence) | | | | CL. + ACET = HCL + R2O2. + HCHO + CCO-O2. + RCO3.+RO2. |
| 1.00E-10 | (No T Dependence) | | | 13 | CL. + MEK = HCL + 0.5 {CCHO + HCHO + CCO-O2. + C2CO-O2.} + RCO3. + 1.5 {R2O2. + RO2.} |
| 1.00E-10 | (No T Dependence) | | | 13 | CL. + RNO3 = HCL + NO2 + 0.155 MEK + 1.05 RCHO + 0.48 CCHO + 0.16 HCHO + 0.11 -C + 1.39 {R2O2. + RO2.} |
| 1.00E-10 | (No T Dependence) | | | 13 | CL. + GLY = HCL + 0.6 HO2. + 1.2 CO + 0.4 {HCOCO-O2. + RCO3.} |
| 1.00E-10 | (No T Dependence) | | | 13 | CL. + MGLY = HCL + CO + CCO-O2. + RCO3. |
| 1.00E-10 | (No T Dependence) | | | | CL. + PHEN = HCL + 0.15 RO2-NP. + 0.85 RO2-R. + 0.2 GLY + 4.7 -C + RO2. |
| 1.00E-10 | (No T Dependence) | | | 13 | CL. + CRES = HCL + 0.15 RO2-NP. + 0.85 RO2-R. + 0.2 MGLY + 5.5 -C + RO2. |
| 1.00E-10 | (No T Dependence) | | | 13 | CL. + BALD = HCL + BZ-CO-O2. + RCO3. |
| 1.00E-10 | (No T Dependence) | | | 13 | CL. + AFG2 = HCL + C2CO-O2. + RCO3. |

[a] A listing of the general mechanism to which these reactions were added is given by Carter *et al.* (1996).

[b] Except as noted, the expression for rate constant is $k = A\ e^{Ea/RT}\ (T/300)^{B}$. Rate constants and A factor are in ppm, min units. Units of Ea is kcal $mole^{-1}$. For falloff kinetics the rate constants are given by $(k0[M]kINF)/(k0[M]+kINF) \times F^{X}$, where $X = 1/(1+\log_{10}(k0[M]/kINF)^{2})$. For photolysis reactions, the rate constants are calculated using the absorption cross sections in the associated photolysis files, which are given below or taken from the latest IUPAC evaluation (Atkinson *et al*, 1996). Unit quantum yields were assumed unless indicated otherwise in the listing.

[c] See Carter (1990) for a description of the species used in the general mechanism.

[d] Documentation notes are as follows. If no documentation notes are given, the kinetic parameters and absorption coefficient and quantum yields are from the latest IUPAC evaluation (Atkinson *et al.*, 1996).

1. The absorption cross sections were obtained in this work as described in the text, and are as follows (given as wavelength in nm, absorption cross section in $cm^2$, base e):

| | | | | | | | | | | | |
|---|---|---|---|---|---|---|---|---|---|---|---|
| 270 | 1.65E-19 | 272 | 1.70E-19 | 274 | 1.73E-19 | 276 | 1.73E-19 | 278 | 1.71E-19 | 280 | 1.67E-19 |
| 282 | 1.62E-19 | 284 | 1.54E-19 | 286 | 1.44E-19 | 288 | 1.34E-19 | 290 | 1.23E-19 | 292 | 1.10E-19 |
| 294 | 9.82E-20 | 296 | 8.71E-20 | 298 | 7.57E-20 | 300 | 6.44E-20 | 302 | 5.47E-20 | 304 | 4.68E-20 |
| 306 | 3.97E-20 | 308 | 3.33E-20 | 310 | 2.79E-20 | 312 | 2.36E-20 | 314 | 2.03E-20 | 316 | 1.77E-20 |
| 318 | 1.55E-20 | 320 | 1.38E-20 | 322 | 1.23E-20 | 324 | 1.10E-20 | 326 | 9.94E-21 | 328 | 8.98E-21 |
| 330 | 8.18E-21 | 332 | 7.54E-21 | 334 | 6.82E-21 | 336 | 6.27E-21 | 338 | 5.69E-21 | 340 | 5.20E-21 |
| 342 | 4.80E-21 | 344 | 4.36E-21 | 346 | 4.00E-21 | 348 | 3.68E-21 | 350 | 3.34E-21 | 352 | 3.05E-21 |
| 354 | 2.70E-21 | 356 | 2.51E-21 | 358 | 2.30E-21 | 360 | 1.54E-21 | 362 | 2.13E-21 | 364 | 1.78E-21 |
| 366 | 1.25E-21 | 368 | 1.28E-21 | 370 | 1.04E-21 | 372 | 1.08E-21 | 374 | 7.13E-22 | 376 | 6.96E-22 |
| 378 | 5.85E-22 | 380 | 5.57E-22 | 382 | 4.66E-22 | 384 | 4.68E-22 | 386 | 1.70E-22 | 388 | 5.02E-22 |
| 390 | 3.50E-22 | 392 | 0.00E+00 | | | | | | | | |

   The total photodecomposion quantum yield, $\Phi_1 + \Phi_2$, was determined to be 0.87±0.26 (see text). Although the data of Moilnanen *et al.* (1976) indicate that $\Phi_2$ is small, the light source they employed may not be representative of that in this work, and two alternative mechanisms, based on differing assumptions concerning the relative importance of the two reaction pathways, are considered.
2. These reaction are only applicable for model 2.
3. Same rate constant as used for other peroxy radical reactions in the general mechanism (Carter, 1990).
4. Calculated using absorption cross sections given in the latest IUPAC tabulation (Atkinson *et al.*, 1996) asuming unit quantum yields.
5. Rate constant from NASA evaluation (NASA, 1994).
6. The kinetic parameters are for the equilibrium constant, which was derived from the low pressure chlorine nitrate decomposition rate constant of Schonle *et al.* (1979), combined with the low pressure rate constant for the reverse reaction.
7. This reaction is neglected because it is of negligible importance compared with the ClO + $NO_x$ and $HO_2$ reactions under the conditions of the simulations discussed here.
8. Rate constants given by Aschmann and Atkinson (1995).
9. Relative rate constant from Atkinson and Aschmann (1985); placed on an absolute basis using the Cl + n-butane rate constant used by Aschmann and Atkinson (1995) for deriving absolute Cl + alkane rate constants. The toluene rate constant is in good agreement with value of Wallington *et al.* (1988).
10. Abstraction from the methyl group is expected to dominate over addition to the aromatic ring, so the representation of the products formed is modified accordingly.
11. Rate constant from Wallington *et al.* (1988).
12. Rate constant estimated from Cl + propene rate constant (Atkinson and Aschmann, 1985) and the estimation method derived for Cl + alkanes (Aschmann and Atkinson, 1995).
13. The rate constants for these organic product + chlorine reaction are unknown and are approximately estimated. They are not expected to be highly important in affecting the results of the simulations because much more of the Cl reacts with the alkanes which are present.

Table 2. Summary of conditions and results of the environmental chamber experiments.

| Run | Initial Concentrations (ppm) | | | | | | Selected Results | | | |
|---|---|---|---|---|---|---|---|---|---|---|
| | Chloro-picrin | NO | $NO_2$ | $Cl_2$ | Other Reactants Type | (ppm) | Time (hrs) | O3 (ppm) | Alkane Reacted[a] | Xylene |
| n-Butane - $NO_x$ (control) | | | | | | | | | | |
| CTC-135 | 0 | 0.20 | 0.06 | 0 | n-Butane | 3.4 | 5 | 0.005 | 2% | - |
| $Cl_2$ - Alkane | | | | | | | | | | |
| CTC-139 | 0 | 0 | 0 | 0.14 | n-Butane | 0.9 | 3 | 0.02 | 26% | - |
| CTC-136 | 0 | 0.29 | 0.11 | 0.14 | n-Butane | 0.9 | 3 | 0.52 | 38% | - |
| Chloropicrin - Alkane | | | | | | | | | | |
| CTC-141A | 1.9 | 0 | 0 | 0 | n-Butane | 1.0 | 5 | 0.81 | 40% | - |
| CTC-141B | 1.9 | 0 | 0 | 0 | | 1.8 | 5 | 0.86 | 25% | - |
| CTC-134A | 2.0 | 0.27 | 0.08 | 0 | Ethane | 0.49 | 5 | 0.46 | 46% | - |
| CTC-134B | 1.9 | 0.27 | 0.08 | 0 | | 0.95 | 5 | 0.50 | 31% | - |
| CTC-125A | 3.1 | 0.21 | 0.05 | 0 | n-Butane | 0.9 | 5 | 0.69 | 36% | - |
| CTC-125B | 3.0 | 0.21 | 0.05 | 0 | | 1.8 | 5 | 0.81 | 23% | - |
| Incremental Reactivity[b] | | | | | | | | | | |
| CTC-112 | 1.9 | 0.22 | 0.07 | 0 | Mini-Surrogate | 4.8 | 5 | 1.01 | 60% | 81% |
| | 0 | 0.21 | 0.07 | 0 | (ppmC)[c] | 4.9 | 5 | 0.20 | 12% | 43% |
| CTC-119 | 0.16 | 0.22 | 0.08 | 0 | | 4.9 | 5 | 0.38 | 19% | 55% |
| | 0 | 0.23 | 0.08 | 0 | | 4.9 | 5 | 0.17 | 10% | 39% |
| CTC-121 | 0.10 | 0.22 | 0.08 | 0 | | 4.8 | 3 | 0.09 | 9% | 32% |
| | 0 | 0.23 | 0.08 | 0 | | 4.8 | 3 | 0.02 | 4% | 19% |
| CTC-126 | 0.25 | 0.28 | 0.10 | 0 | Full Surrogate | 5.4 | 5 | 0.40 | 12% | 59% |
| | 0 | 0.28 | 0.10 | 0 | (ppmC)[d] | 5.4 | 5 | 0.27 | 6% | 52% |
| CTC-124 | 0.15 | 0.27 | 0.11 | 0 | | 5.7 | 5 | 0.35 | 11% | 57% |
| | 0 | 0.28 | 0.11 | 0 | | 5.5 | 5 | 0.28 | 8% | 54% |

[a] Percent reduction of the alkane or m-xylene concentration during the time period indicated . Alkane refers either to the alkane in the "other reactants" column, n-heane for the mini-surrogate experiments, or n-butane for the full surrogate runs..

[b] In these experiments, equal amounts of all the reactants except chloropicrin were injected into both of the dual chambers, and clhoropicrin was injected into one but not the other.

[c] The mini-surrogate components, and their average concentrations in these experiments, were as follows: n-hexane: 0.43 ppm; ethylene: 0.67 ppm; and m-xylene: 0.13 ppm.

[d] The full surrogate components, and their average concentrations in these experiments, were as follows: n-butane: 0.47 ppm; n-octane: 0.13 ppm; ethene: 0.092 ppm; propene: 0.065 ppm; trans-2-butene: 0.061 ppm; toluene: 0.12 ppm; m-xylene: 0.12 ppm; formaldehyde: 0.10 ppm.

Table 3. Results of relative atmospheric ozone impact estimates for chloropicrin and other representative VOCs for the three averaged conditions scenarios.

| Compound | Relative Reactivity[a] (mass basis) | | |
|---|---|---|---|
| | Max React | Max $O_3$ | Low $NO_x$ |
| Chloropicrin | | | |
| Model 1 | 0.28 | 0.47 | 1.14 |
| Model 2 | 0.41 | 0.65 | 1.42 |
| Other VOCs | | | |
| Ethane | 0.08 | 0.15 | 0.19 |
| n-Butane | 0.32 | 0.61 | 0.75 |
| n-Octane | 0.22 | 0.42 | 0.40 |
| Ethene | 2.1 | 2.3 | 2.6 |
| Propene | 2.7 | 2.9 | 3.4 |
| trans-2-butene | 3.3 | 3.1 | 3.6 |
| Toluene | 1.2 | 0.77 | 0.14 |
| M-Xylene | 3.6 | 2.8 | 2.4 |
| Formaldehyde | 1.7 | 1.16 | 1.03 |
| Acetone | 0.12 | 0.13 | 0.14 |

[a] Incremental reactivity of the compound divided by the emissions-weighted average incremental reactivity of all reactive organic gas emissions.

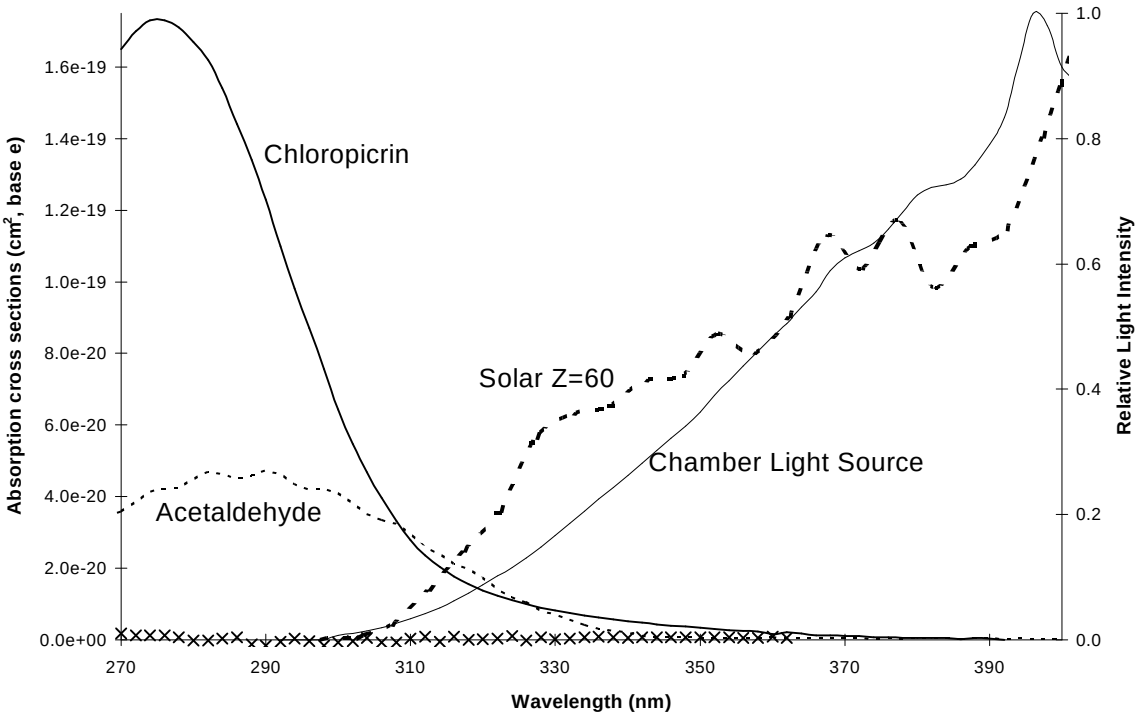


Figure 1. Absorption cross sections for chloropicrin and acetaldehyde and relative light intensities for ground level sunlight and for the chamber light source. The "x"'s show the differences between the acetaldehyde absorption cross sections measured in this work and the IUPAC (1996) recommended values. The light intensities are in arbitrary units normalized so that each yields the same $NO_2$ photolysis rate.

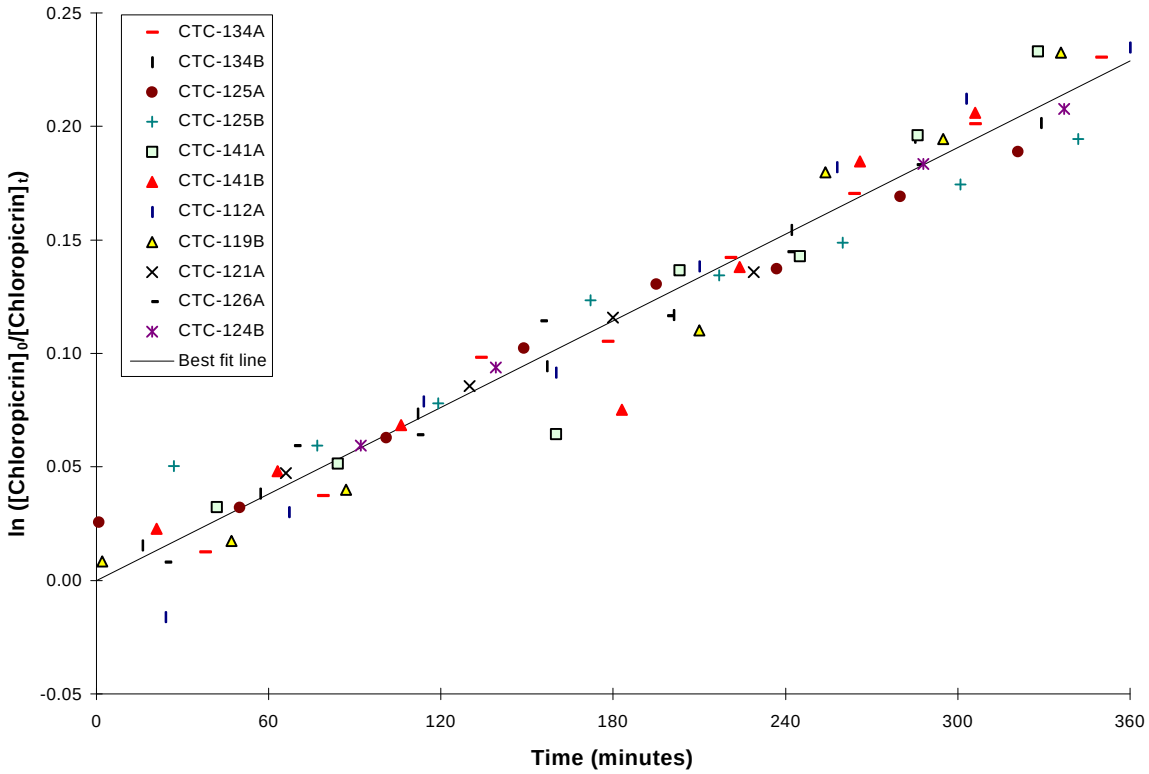


Figure 2. Plots of $\ln([\text{Chloropicrin}]_0/[\text{Chloropicrin}]_t)$ vs time for all the environmental chamber experiments.

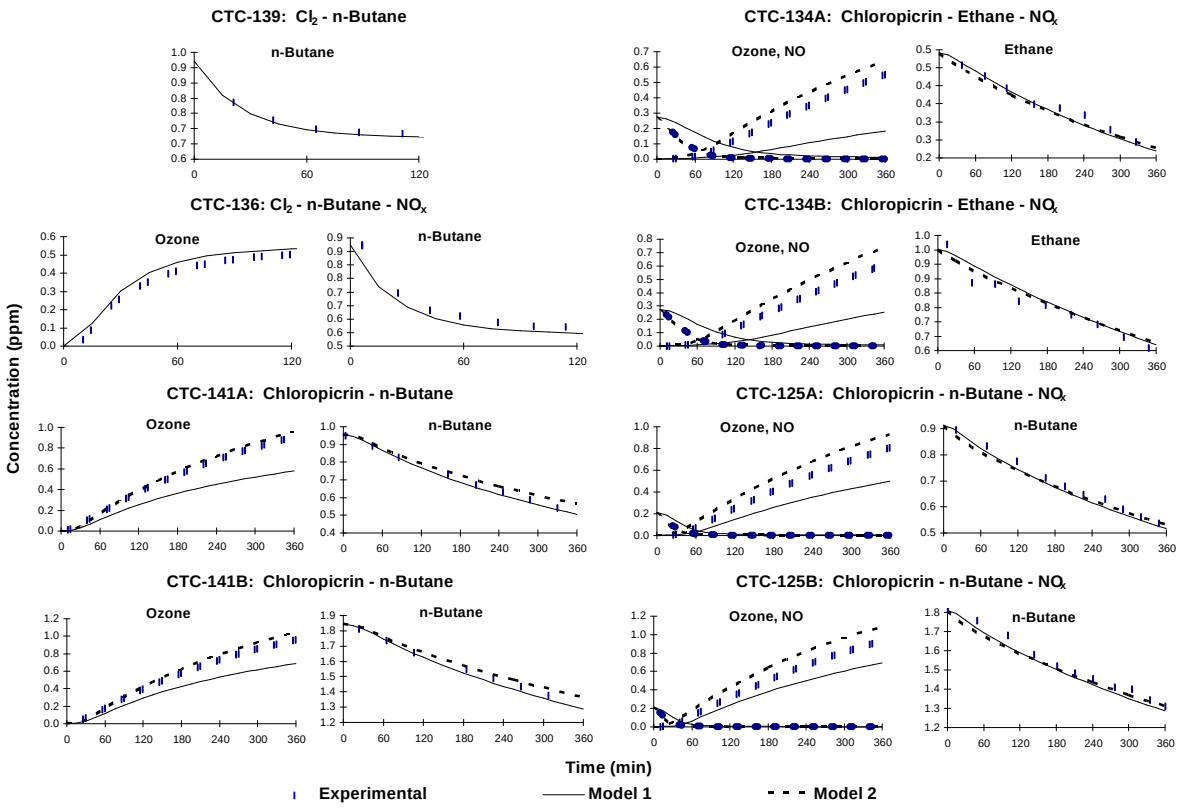


Figure 3. Selected experimental and calculated results from the $Cl_2$ - alkane and chloropicrin - alkane chamber experiments.

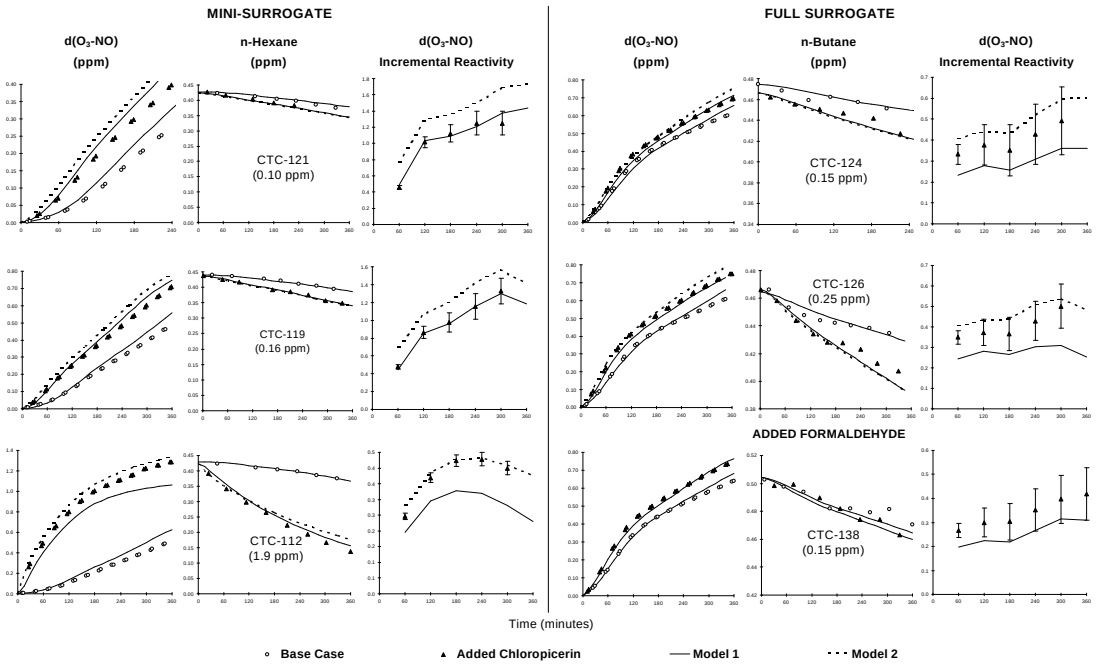


Figure 4. Selected experimental and calculated results for the incremental reactivity experiments. Results of a comparable formaldehyde reactivity experiment are also shown.

## APPENDIX A
## LISTING OF THE GENERAL ATMOSPHERIC PHOTOOXIDATION MECHANISM

This Appendix contains a complete listing of the chemical mechanism used in the environmental chamber and atmospheric reactivity simulations discussed in this report, except for the reactions of chlorpicrin, Cl atoms, and other chlorine-containing products, which are given in Table 1 of the main report. Table A-1 lists the species used in the general mechanism, and Table A-2 lists the reactions and the rate constants. Footnotes to Table A-2 indicate the nomenclature used. Table A-3 lists the absorption cross sections and quantum yields for the photolysis reactions in the general mechanism, and Table A-4 lists the values for the chamber-dependent parameters used in the model simulations of the environmental chamber experiments, and gives brief explanations of the values used.

Table A-1. List of species in the chemical mechanism used in the model simulations for this study.

| Name | Description |
|---|---|
| **Constant Species.** | |
| O2 | Oxygen |
| M | Air |
| H2O | Water |
| **Active Inorganic Species.** | |
| O3 | Ozone |
| NO | Nitric Oxide |
| NO2 | Nitrogen Dioxide |
| NO3 | Nitrate Radical |
| N2O5 | Nitrogen Pentoxide |
| HONO | Nitrous Acid |
| HNO3 | Nitric Acid |
| HNO4 | Peroxynitric Acid |
| HO2H | Hydrogen Peroxide |
| **Active Radical Species and Operators.** | |
| HO2. | Hydroperoxide Radicals |
| RO2. | Operator to Calculate Total Organic Peroxy Radicals |
| RCO3. | Operator to Calculate Total Acetyl Peroxy Radicals |

Table A-1 (continued)

| Name | Description |
|---|---|
| **Active Reactive Organic Product Species.** | |
| CO | Carbon Monoxide |
| HCHO | Formaldehyde |
| CCHO | Acetaldehyde |
| RCHO | Lumped C3+ Aldehydes |
| ACET | Acetone |
| MEK | Lumped Ketones |
| PHEN | Phenol |
| CRES | Cresols |
| BALD | Aromatic aldehydes (e.g., benzaldehyde) |
| GLY | Glyoxal |
| MGLY | Methyl Glyoxal |
| AFG1 | Reactive Aromatic Fragmentation Products from benzene and naphthalene |
| AFG2 | Other Reactive Aromatic Fragmentation Products |
| AFG3 | Aromatic Fragmentation Products used in adjusted m-xylene mechanism |
| RNO3 | Organic Nitrates |
| NPHE | Nitrophenols |
| ISOPROD | Lumped isoprene product species |
| PAN | Peroxy Acetyl Nitrate |
| PPN | Peroxy Propionyl Nitrate |
| GPAN | PAN Analogue formed from Glyoxal |
| PBZN | PAN Analogues formed from Aromatic Aldehydes |
| -OOH | Operator Representing Hydroperoxy Groups |
| **Non-Reacting Species** | |
| CO2 | Carbon Dioxide |
| -C | "Lost Carbon" |
| -N | "Lost Nitrogen" |
| H2 | Hydrogen |
| **Steady State Species and Operators.** | |
| HO. | Hydroxyl Radicals |
| O | Ground State Oxygen Atoms |
| O*1D2 | Excited Oxygen Atoms |
| RO2-R. | Peroxy Radical Operator representing NO to $NO_2$ conversion with $HO_2$ formation. |
| RO2-N. | Peroxy Radical Operator representing NO consumption with organic nitrate formation. |
| RO2-NP. | Peroxy Radical Operator representing NO consumption with nitrophenol formation |
| R2O2. | Peroxy Radical Operator representing NO to $NO_2$ conversion. |
| CCO-O2. | Peroxy Acetyl Radicals |
| C2CO-O2. | Peroxy Propionyl Radicals |
| HCOCO-O2. | Peroxyacyl Radical formed from Glyoxal |
| BZ-CO-O2. | Peroxyacyl Radical formed from Aromatic Aldehydes |
| HOCOO. | Intermediate formed in Formaldehyde + $HO_2$ reaction |

Table A-1 (continued)

| Name | Description |
|---|---|
| BZ-O. | Phenoxy Radicals |
| BZ(NO2)-O. | Nitratophenoxy Radicals |
| HOCOO. | Radical Intermediate formed in the $HO_2$ + Formaldehyde system. |
| (HCHO2) | Excited Criegee biradicals formed from $=CH_2$ groups |
| (CCHO2) | Excited Criegee biradicals formed from $=CHCH_3$ groups |
| (RCHO2) | Excited Criegee biradicals formed from =CHR groups, where R not $CH_3$ |
| (C(C)CO2) | Excited Criegee biradicals formed from $=C(CH_3)_2$ groups |
| (C(R)CO2) | Excited Criegee biradicals formed from $=C(CH_3)R$ or $CR_2$ groups |
| (BZCHO2) | Excited Criegee biradicals formed from styrenes |
| **Hydrocarbon species represented explicitly** | |
| CH4 | Methane (EKMA simulations only) |
| ETHANE | Ethane (Ethane reactivity simulations only) |
| N-C4 | n-Butane (Chamber simulations only) |
| N-C6 | n-Hexane (Chamber simulations only) |
| N-C8 | n-Octane (Chamber simulations only) |
| ETHE | Ethene |
| ISOP | Isoprene (EKMA Simulations only) |
| APIN | α-Pinene (EKMA Simulations only) |
| UNKN | Unknown biogenics. (EKMA Simulations only) |
| PROPENE | Propene (Chamber simulations only) |
| T-2-BUTE | trans-2-Butene (Chamber simulations only) |
| TOLUENE | Toluene (Chamber simulations only) |
| M-XYLENE | m-Xylene (Chamber simulations only) |
| **Lumped species used to represent the Base ROG mixture in the EKMA model simulations.** | |
| ALK1 | Alkanes and other saturated compounds with $k_{OH} < 10^4$ $ppm^{-1}$ $min^{-1}$. |
| ALK2 | Alkanes and other saturated compounds with $k_{OH} \geq 10^4$ $ppm^{-1}$ $min^{-1}$. |
| ARO1 | Aromatics with $k_{OH} < 2x10^4$ $ppm^{-1}$ $min^{-1}$. |
| ARO2 | Aromatics with $k_{OH} \geq 2x10^4$ $ppm^{-1}$ $min^{-1}$. |
| OLE2 | Alkenes (other than ethene) with $k_{OH} < 7x10^4$ $ppm^{-1}$ $min^{-1}$. |
| OLE3 | Alkenes with $k_{OH} \geq 7x10^4$ $ppm^{-1}$ $min^{-1}$. |

Table A-2. List of reactions in the geneneral chemical mechanism used in the model simulations for this study. [a]

| Rxn. Label | Kinetic Parameters [b] k(300) | A | Ea | B | Reactions [c] |
|---|---|---|---|---|---|
| **Inorganic Reactions** | | | | | |
| 1 | (Phot. File = NO2 ) | | | | NO2 + HV = NO + O |
| 2 | 6.00E-34 | 6.00E-34 | 0.00 | -2.30 | O + O2 + M = O3 + M |
| 3A | 9.69E-12 | 6.50E-12 | -0.24 | 0.00 | O + NO2 = NO + O2 |
| 3B | 8.98E-26 | (Falloff Kinetics) | | | O + NO2 = NO3 + M |
| | k0 = | 9.00E-32 | 0.00 | -2.00 | |
| | kINF = | 2.20E-11 | 0.00 | 0.00 | |
| | | F= 0.60 | n= 1.00 | | |
| 4 | 1.88E-14 | 2.00E-12 | 2.78 | 0.00 | O3 + NO = NO2 + O2 |
| 5 | 3.36E-17 | 1.40E-13 | 4.97 | 0.00 | O3 + NO2 = O2 + NO3 |
| 6 | 2.80E-11 | 1.70E-11 | -0.30 | 0.00 | NO + NO3 = 2 NO2 |
| 7 | 1.92E-38 | 3.30E-39 | -1.05 | 0.00 | NO + NO + O2 = 2 NO2 |
| 8 | 2.19E-24 | (Falloff Kinetics) | | | NO2 + NO3 = N2O5 |
| | k0 = | 2.20E-30 | 0.00 | -4.30 | |
| | kINF = | 1.50E-12 | 0.00 | -0.50 | |
| | | F= 0.60 | n= 1.00 | | |
| 9 | 5.53E+10 | 9.09E+26 | 22.26 | 0.00 | N2O5 + #RCON8 = NO2 + NO3 |
| 10 | 1.00E-21 | (No T Dependence) | | | N2O5 + H2O = 2 HNO3 |
| 11 | 4.17E-16 | 2.50E-14 | 2.44 | 0.00 | NO2 + NO3 = NO + NO2 + O2 |
| 12A | (Phot. File = NO3NO ) | | | | NO3 + HV = NO + O2 |
| 12B | (Phot. File = NO3NO2 ) | | | | NO3 + HV = NO2 + O |
| 13A | (Phot. File = O3O3P ) | | | | O3 + HV = O + O2 |
| 13B | (Phot. File = O3O1D ) | | | | O3 + HV = O*1D2 + O2 |
| 14 | 2.20E-10 | (No T Dependence) | | | O*1D2 + H2O = 2 HO. |
| 15 | 2.92E-11 | 1.92E-11 | -0.25 | 0.00 | O*1D2 + M = O + M |
| 16 | 6.98E-25 | (Falloff Kinetics) | | | HO. + NO = HONO |
| | k0 = | 7.00E-31 | 0.00 | -2.60 | |
| | kINF = | 1.50E-11 | 0.00 | -0.50 | |
| | | F= 0.60 | n= 1.00 | | |
| 17 | (Phot. File = HONO ) | | | | HONO + HV = HO. + NO |
| 18 | 2.59E-24 | (Falloff Kinetics) | | | HO. + NO2 = HNO3 |
| | k0 = | 2.60E-30 | 0.00 | -3.20 | |
| | kINF = | 2.40E-11 | 0.00 | -1.30 | |
| | | F= 0.60 | n= 1.00 | | |
| 19 | 1.03E-13 | 6.45E-15 | -1.65 | 0.00 | HO. + HNO3 = H2O + NO3 |
| 21 | 2.40E-13 | (No T Dependence) | | | HO. + CO = HO2. + CO2 |
| 22 | 6.95E-14 | 1.60E-12 | 1.87 | 0.00 | HO. + O3 = HO2. + O2 |
| 23 | 8.28E-12 | 3.70E-12 | -0.48 | 0.00 | HO2. + NO = HO. + NO2 |
| 24 | 1.79E-25 | (Falloff Kinetics) | | | HO2. + NO2 = HNO4 |
| | k0 = | 1.80E-31 | 0.00 | -3.20 | |
| | kINF = | 4.70E-12 | 0.00 | -1.40 | |
| | | F= 0.60 | n= 1.00 | | |
| 25 | 7.92E+10 | 4.76E+26 | 21.66 | 0.00 | HNO4 + #RCON24 = HO2. + NO2 |
| 27 | 4.61E-12 | 1.30E-12 | -0.75 | 0.00 | HNO4 + HO. = H2O + NO2 + O2 |
| 28 | 2.08E-15 | 1.10E-14 | 0.99 | 0.00 | HO2. + O3 = HO. + 2 O2 |
| 29A | 1.73E-12 | 2.20E-13 | -1.23 | 0.00 | HO2. + HO2. = HO2H + O2 |
| 29B | 5.00E-32 | 1.90E-33 | -1.95 | 0.00 | HO2. + HO2. + M = HO2H + O2 |
| 29C | 3.72E-30 | 3.10E-34 | -5.60 | 0.00 | HO2. + HO2. + H2O = HO2H + O2 + H2O |
| 29D | 2.65E-30 | 6.60E-35 | -6.32 | 0.00 | HO2. + HO2. + H2O = HO2H + O2 + H2O |
| 30A | 1.73E-12 | 2.20E-13 | -1.23 | 0.00 | NO3 + HO2. = HNO3 + O2 |
| 30B | 5.00E-32 | 1.90E-33 | -1.95 | 0.00 | NO3 + HO2. + M = HNO3 + O2 |
| 30C | 3.72E-30 | 3.10E-34 | -5.60 | 0.00 | NO3 + HO2. + H2O = HNO3 + O2 + H2O |
| 30D | 2.65E-30 | 6.60E-35 | -6.32 | 0.00 | NO3 + HO2. + H2O = HNO3 + O2 + H2O |
| 31 | (Phot. File = H2O2 ) | | | | HO2H + HV = 2 HO. |
| 32 | 1.70E-12 | 3.30E-12 | 0.40 | 0.00 | HO2H + HO. = HO2. + H2O |
| 33 | 9.90E-11 | 4.60E-11 | -0.46 | 0.00 | HO. + HO2. = H2O + O2 |
| **Peroxy Radical Operators** | | | | | |
| B1 | 7.68E-12 | 4.20E-12 | -0.36 | 0.00 | RO2. + NO = NO |
| B2 | 5.59E-22 | (Falloff Kinetics) | | | RCO3. + NO = NO |
| | k0 = | 5.65E-28 | 0.00 | -7.10 | |
| | kINF = | 2.64E-11 | 0.00 | -0.90 | |
| | | F= 0.27 | n= 1.00 | | |
| B4 | 2.54E-22 | (Falloff Kinetics) | | | RCO3. + NO2 = NO2 |
| | k0 = | 2.57E-28 | 0.00 | -7.10 | |
| | kINF = | 1.20E-11 | 0.00 | -0.90 | |
| | | F= 0.30 | n= 1.00 | | |
| B5 | 4.90E-12 | 3.40E-13 | -1.59 | 0.00 | RO2. + HO2. = HO2. + RO2-HO2-PROD |
| B6 | 4.90E-12 | 3.40E-13 | -1.59 | 0.00 | RCO3. + HO2. = HO2. + RO2-HO2-PROD |

Table A-2 (continued)

| Rxn. Label | Kinetic Parameters [b] k(300) | A | Ea | B | Reactions [c] |
|---|---|---|---|---|---|
| B8 | 1.00E-15 | (No T Dependence) | | | RO2. + RO2. = RO2-RO2-PROD |
| B9 | 1.09E-11 | 1.86E-12 | -1.05 | 0.00 | RO2. + RCO3. = RO2-RO2-PROD |
| B10 | 1.64E-11 | 2.80E-12 | -1.05 | 0.00 | RCO3. + RCO3. = RO2-RO2-PROD |
| B11 | (Same k as for RO2. ) | | | | RO2-R. + NO = NO2 + HO2. |
| B12 | (Same k as for RO2. ) | | | | RO2-R. + HO2. = -OOH |
| B13 | (Same k as for RO2. ) | | | | RO2-R. + RO2. = RO2. + 0.5 HO2. |
| B14 | (Same k as for RO2. ) | | | | RO2-R. + RCO3. = RCO3. + 0.5 HO2. |
| B19 | (Same k as for RO2. ) | | | | RO2-N. + NO = RNO3 |
| B20 | (Same k as for RO2. ) | | | | RO2-N. + HO2. = -OOH + MEK + 1.5 -C |
| B21 | (Same k as for RO2. ) | | | | RO2-N. + RO2. = RO2. + 0.5 HO2. + MEK + 1.5 -C |
| B22 | (Same k as for RO2. ) | | | | RO2-N. + RCO3. = RCO3. + 0.5 HO2. + MEK + 1.5 -C |
| B15 | (Same k as for RO2. ) | | | | R2O2. + NO = NO2 |
| B16 | (Same k as for RO2. ) | | | | R2O2. + HO2. = |
| B17 | (Same k as for RO2. ) | | | | R2O2. + RO2. = RO2. |
| B18 | (Same k as for RO2. ) | | | | R2O2. + RCO3. = RCO3. |
| B23 | (Same k as for RO2. ) | | | | RO2-XN. + NO = -N |
| B24 | (Same k as for RO2. ) | | | | RO2-XN. + HO2. = -OOH |
| B25 | (Same k as for RO2. ) | | | | RO2-XN. + RO2. = RO2. + 0.5 HO2. |
| B26 | (Same k as for RO2. ) | | | | RO2-XN. + RCO3. = RCO3. + HO2. |
| G2 | (Same k as for RO2. ) | | | | RO2-NP. + NO = NPHE |
| G3 | (Same k as for RO2. ) | | | | RO2-NP. + HO2. = -OOH + 6 -C |
| G4 | (Same k as for RO2. ) | | | | RO2-NP. + RO2. = RO2. + 0.5 HO2. + 6 -C |
| G5 | (Same k as for RO2. ) | | | | RO2-NP. + RCO3. = RCO3. + HO2. + 6 -C |
| **Excited Criegee Biradicals** | | | | | |
| RZ1 | (fast) | | | | (HCHO2) = 0.7 HCOOH + 0.12 "HO. + HO2. + CO" + 0.18 "H2 + CO2" |
| RZ2 | (fast) | | | | (CCHO2) = 0.25 CCOOH + 0.15 "CH4 + CO2" + 0.6 HO. + 0.3 "CCO-O2. + RCO3." + 0.3 "RO2-R. + HCHO + CO + RO2." |
| RZ3 | (fast) | | | | (RCHO2) = 0.25 CCOOH + 0.15 CO2 + 0.6 HO. + 0.3 "C2CO-O2. + RCO3." + 0.3 "RO2-R. + CCHO + CO + RO2." + 0.55 -C |
| RZ4 | (fast) | | | | (C(C)CO2) = HO. + R2O2. + HCHO + CCO-O2. + RCO3. + RO2. |
| RZ5 | (fast) | | | | (C(R)CO2) = HO. + CCO-O2. + CCHO + R2O2. + RCO3. + RO2. |
| RZ6 | (fast) | | | | (CYCCO2) = 0.3 "HO. + C2CO-O2. + R2O2. + RCO3. + RO2." + 0.3 RCHO + 4.2 -C |
| RZ8 | (fast) | | | | (BZCHO2) = 0.5 "BZ-O. + R2O2. + CO + HO." |
| ISZ1 | (fast) | | | | (C:CC(C)O2) = HO. + R2O2. + HCHO + C2CO-O2. + RO2. + RCO3. |
| ISZ2 | (fast) | | | | (C:C(C)CHO2) = 0.75 RCHO + 0.25 ISOPROD + 0.5 -C |
| MAZ1 | (fast) | | | | (C2(O2)CHO) = HO. + R2O2. + HCHO + HCOCO-O2. + RO2. + RCO3. |
| M1Z1 | (fast) | | | | (HOCCHO2) = 0.6 HO. + 0.3 "CCO-O2. + RCO3." + 0.3 "RO2-R. + HCHO + CO + RO2." + 0.8 -C |
| M2Z1 | (fast) | | | | (HCOCHO2) = 0.12 "HO2. + 2 CO + HO." + 0.74 -C + 0.51 "CO2 + HCHO" |
| M2Z2 | (fast) | | | | (C2(O2)COH) = HO. + MGLY + HO2. + R2O2. + RO2. |
| **Organic Product Species** | | | | | |
| B7 | (Phot. File = CO2H ) | | | | -OOH + HV = HO2. + HO. |
| B7A | 1.81E-12 | 1.18E-12 | -0.25 | 0.00 | HO. + -OOH = HO. |
| B7B | 3.71E-12 | 1.79E-12 | -0.44 | 0.00 | HO. + -OOH = RO2-R. + RO2. |
| C1 | (Phot. File = HCHONEWR) | | | | HCHO + HV = 2 HO2. + CO |
| C2 | (Phot. File = HCHONEWM) | | | | HCHO + HV = H2 + CO |
| C3 | 9.76E-12 | 1.13E-12 | -1.29 | 2.00 | HCHO + HO. = HO2. + CO + H2O |
| C4 | 7.79E-14 | 9.70E-15 | -1.24 | 0.00 | HCHO + HO2. = HOCOO. |
| C4A | 1.77E+02 | 2.40E+12 | 13.91 | 0.00 | HOCOO. = HO2. + HCHO |
| C4B | (Same k as for RO2. ) | | | | HOCOO. + NO = -C + NO2 + HO2. |
| C9 | 6.38E-16 | 2.80E-12 | 5.00 | 0.00 | HCHO + NO3 = HNO3 + HO2. + CO |
| C10 | 1.57E-11 | 5.55E-12 | -0.62 | 0.00 | CCHO + HO. = CCO-O2. + H2O + RCO3. |
| C11A | (Phot. File = CCHOR ) | | | | CCHO + HV = CO + HO2. + HCHO + RO2-R. + RO2. |
| C12 | 2.84E-15 | 1.40E-12 | 3.70 | 0.00 | CCHO + NO3 = HNO3 + CCO-O2. + RCO3. |
| C25 | 1.97E-11 | 8.50E-12 | -0.50 | 0.00 | RCHO + HO. = C2CO-O2. + RCO3. |
| C26 | (Phot. File = RCHO ) | | | | RCHO + HV = CCHO + RO2-R. + RO2. + CO + HO2. |
| C27 | 2.84E-15 | 1.40E-12 | 3.70 | 0.00 | NO3 + RCHO = HNO3 + C2CO-O2. + RCO3. |

Table A-2 (continued)

| Rxn. Label | Kinetic Parameters [b] k(300) | A | Ea | B | Reactions [c] |
|---|---|---|---|---|---|
| C38 | 2.23E-13 | 4.81E-13 | 0.46 | 2.00 | ACET + HO. = R2O2. + HCHO + CCO-O2. + RCO3. + RO2. |
| C39 | (Phot. File = ACET-93C) | | | | ACET + HV = CCO-O2. + HCHO + RO2-R. + RCO3. + RO2. |
| C44 | 1.16E-12 | 2.92E-13 | -0.82 | 2.00 | MEK + HO. = H2O + 0.5 "CCHO + HCHO + CCO-O2. + C2CO-O2." + RCO3. + 1.5 "R2O2. + RO2." |
| C57 | (Phot. File = KETONE ) | | | | MEK + HV + #0.1 = CCO-O2. + CCHO + RO2-R. + RCO3. + RO2. |
| C95 | 2.07E-12 | 2.19E-11 | 1.41 | 0.00 | RNO3 + HO. = NO2 + 0.155 MEK + 1.05 RCHO + 0.48 CCHO + 0.16 HCHO + 0.11 -C + 1.39 "R2O2. + RO2." |
| C58A | (Phot. File = GLYOXAL1) | | | | GLY + HV = 0.8 HO2. + 0.45 HCHO + 1.55 CO |
| C58B | (Phot. File = GLYOXAL2) | | | | GLY + HV + #0.029 = 0.13 HCHO + 1.87 CO |
| C59 | 1.14E-11 | (No T Dependence) | | | GLY + HO. = 0.6 HO2. + 1.2 CO + 0.4 "HCOCO-O2. + RCO3." |
| C60 | (Same k as for CCHO ) | | | | GLY + NO3 = HNO3 + 0.6 HO2. + 1.2 CO + 0.4 "HCOCO-O2. + RCO3." |
| C68A | (Phot. File = MEGLYOX1) | | | | MGLY + HV = HO2. + CO + CCO-O2. + RCO3. |
| C68B | (Phot. File = MEGLYOX2) | | | | MGLY + HV + 0.107 = HO2. + CO + CCO-O2. + RCO3. |
| C69 | 1.72E-11 | (No T Dependence) | | | MGLY + HO. = CO + CCO-O2. + RCO3. |
| C70 | (Same k as for CCHO ) | | | | MGLY + NO3 = HNO3 + CO + CCO-O2. + RCO3. |
| G7 | 1.14E-11 | (No T Dependence) | | | HO. + AFG1 = HCOCO-O2. + RCO3. |
| G8 | (Phot. File = ACROLEIN) | | | | AFG1 + HV + #0.029 = HO2. + HCOCO-O2. + RCO3. |
| U2OH | 1.72E-11 | (No T Dependence) | | | HO. + AFG2 = C2CO-O2. + RCO3. |
| U2HV | (Phot. File = ACROLEIN) | | | | AFG2 + HV = HO2. + CO + CCO-O2. + RCO3. |
| G46 | 2.63E-11 | (No T Dependence) | | | HO. + PHEN = 0.15 RO2-NP. + 0.85 RO2-R. + 0.2 GLY + 4.7 -C + RO2. |
| G51 | 3.60E-12 | (No T Dependence) | | | NO3 + PHEN = HNO3 + BZ-O. |
| G52 | 4.20E-11 | (No T Dependence) | | | HO. + CRES = 0.15 RO2-NP. + 0.85 RO2-R. + 0.2 MGLY + 5.5 -C + RO2. |
| G57 | 2.10E-11 | (No T Dependence) | | | NO3 + CRES = HNO3 + BZ-O. + -C |
| G30 | 1.29E-11 | (No T Dependence) | | | BALD + HO. = BZ-CO-O2. + RCO3. |
| G31 | (Phot. File = BZCHO ) | | | | BALD + HV + #0.05 = 7 -C |
| G32 | 2.61E-15 | 1.40E-12 | 3.75 | 0.00 | BALD + NO3 = HNO3 + BZ-CO-O2. |
| G58 | 3.60E-12 | (No T Dependence) | | | NPHE + NO3 = HNO3 + BZ(NO2)-O. |
| G59 | (Same k as for BZ-O. ) | | | | BZ(NO2)-O. + NO2 = 2 -N + 6 -C |
| G60 | (Same k as for RO2. ) | | | | BZ(NO2)-O. + HO2. = NPHE |
| G61 | (Same k as for BZ-O. ) | | | | BZ(NO2)-O. = NPHE |
| C13 | (Same k as for RCO3. ) | | | | CCO-O2. + NO = CO2 + NO2 + HCHO + RO2-R. + RO2. |
| C14 | (Same k as for RCO3. ) | | | | CCO-O2. + NO2 = PAN |
| C15 | (Same k as for RCO3. ) | | | | CCO-O2. + HO2. = -OOH + CO2 + HCHO |
| C16 | (Same k as for RCO3. ) | | | | CCO-O2. + RO2. = RO2. + 0.5 HO2. + CO2 + HCHO |
| C17 | (Same k as for RCO3. ) | | | | CCO-O2. + RCO3. = RCO3. + HO2. + CO2 + HCHO |
| C18 | 1.67E-14 | (Falloff Kinetics) | | | PAN = CCO-O2. + NO2 + RCO3. |
| | k0 = | 4.90E-03 | 23.97 | 0.00 | |
| | kINF = | 4.00E+16 | 27.08 | 0.00 | |
| | | F= 0.30 | n= 1.00 | | |
| C28 | (Same k as for RCO3. ) | | | | C2CO-O2. + NO = CCHO + RO2-R. + CO2 + NO2 + RO2. |
| C29 | 8.40E-12 | (No T Dependence) | | | C2CO-O2. + NO2 = PPN |
| C30 | (Same k as for RCO3. ) | | | | C2CO-O2. + HO2. = -OOH + CCHO + CO2 |
| C31 | (Same k as for RCO3. ) | | | | C2CO-O2. + RO2. = RO2. + 0.5 HO2. + CCHO + CO2 |
| C32 | (Same k as for RCO3. ) | | | | C2CO-O2. + RCO3. = RCO3. + HO2. + CCHO + CO2 |
| C33 | 6.78E-04 | 1.60E+17 | 27.97 | 0.00 | PPN = C2CO-O2. + NO2 + RCO3. |
| C62 | (Same k as for RCO3. ) | | | | HCOCO-O2. + NO = NO2 + CO2 + CO + HO2. |
| C63 | (Same k as for RCO3. ) | | | | HCOCO-O2. + NO2 = GPAN |
| C65 | (Same k as for RCO3. ) | | | | HCOCO-O2. + HO2. = -OOH + CO2 + CO |
| C66 | (Same k as for RCO3. ) | | | | HCOCO-O2. + RO2. = RO2. + 0.5 HO2. + CO2 + CO |
| C67 | (Same k as for RCO3. ) | | | | HCOCO-O2. + RCO3. = RCO3. + HO2. + CO2 + CO |
| C64 | (Same k as for PAN ) | | | | GPAN = HCOCO-O2. + NO2 + RCO3. |
| G33 | (Same k as for RCO3. ) | | | | BZ-CO-O2. + NO = BZ-O. + CO2 + NO2 + R2O2. + RO2. |
| G43 | 3.53E-11 | 1.30E-11 | -0.60 | 0.00 | BZ-O. + NO2 = NPHE |
| G44 | (Same k as for RO2. ) | | | | BZ-O. + HO2. = PHEN |
| G45 | 1.00E-03 | (No T Dependence) | | | BZ-O. = PHEN |
| G34 | 8.40E-12 | (No T Dependence) | | | BZ-CO-O2. + NO2 = PBZN |
| G36 | (Same k as for RCO3. ) | | | | BZ-CO-O2. + HO2. = -OOH + CO2 + PHEN |

Table A-2 (continued)

| Rxn. Label | Kinetic Parameters [b] k(300) | A | Ea | B | Reactions [c] |
|---|---|---|---|---|---|
| G37 | (Same k as for RCO3. ) | | | | BZ-CO-O2. + RO2. = RO2. + 0.5 HO2. + CO2 + PHEN |
| G38 | (Same k as for RCO3. ) | | | | BZ-CO-O2. + RCO3. = RCO3. + HO2. + CO2 + PHEN |
| G35 | 2.17E-04 | 1.60E+15 | 25.90 | 0.00 | PBZN = BZ-CO-O2. + NO2 + RCO3. |
| IPOH | 3.36E-11 | (No T Dependence) | | | ISOPROD + HO. = 0.293 CO + 0.252 CCHO + 0.126 HCHO + 0.041 GLY + 0.021 RCHO + 0.168 MGLY + 0.314 MEK + 0.503 RO2-R. + 0.21 CCO-O2. + 0.288 C2CO-O2. + 0.21 R2O2. + 0.713 RO2. + 0.498 RCO3. + -0.112 -C |
| IPO3 | 7.11E-18 | (No T Dependence) | | | ISOPROD + O3 = 0.02 CCHO + 0.04 HCHO + 0.01 GLY + 0.84 MGLY + 0.09 MEK + 0.66 (HCHO2) + 0.09 (HCOCHO2) + 0.18 (HOCCHO2) + 0.06 (C2(O2)CHO) + 0.01 (C2(O2)COH) + -0.39 -C |
| IPHV | (Phot. File = ACROLEIN) | | | | ISOPROD + HV + 0.0036 = 0.333 CO + 0.067 CCHO + 0.9 HCHO + 0.033 MEK + 0.333 HO2. + 0.7 RO2-R. + 0.267 CCO-O2. + 0.7 C2CO-O2. + 0.7 RO2. + 0.967 RCO3. + -0.133 -C |
| IPN3 | 1.00E-15 | (No T Dependence) | | | ISOPROD + NO3 = 0.643 CO + 0.282 HCHO + 0.85 RNO3 + 0.357 RCHO + 0.925 HO2. + 0.075 C2CO-O2. + 0.075 R2O2. + 0.925 RO2. + 0.075 RCO3. + 0.075 HNO3 + -2.471 -C |
| **Hydrocarbon Species Represented Explicitly** | | | | | |
| | 2.56E-12 | 1.36E-12 | -0.38 | 2.00 | N-C4 + HO. = 0.076 RO2-N. + 0.924 RO2-R. + 0.397 R2O2. + 0.001 HCHO + 0.571 CCHO + 0.14 RCHO + 0.533 MEK + -0.076 -C + 1.397 RO2. |
| | 5.63E-12 | 1.35E-11 | 0.52 | 0.00 | N-C6 + HO. = 0.185 RO2-N. + 0.815 RO2-R. + 0.738 R2O2. + 0.02 CCHO + 0.105 RCHO + 1.134 MEK + 0.186 -C + 1.738 RO2. |
| | 8.76E-12 | 3.15E-11 | 0.76 | 0.00 | N-C8 + HO. = 0.333 RO2-N. + 0.667 RO2-R. + 0.706 R2O2. + 0.002 RCHO + 1.333 MEK + 0.998 -C + 1.706 RO2. |
| | 8.43E-12 | 1.96E-12 | -0.87 | 0.00 | ETHENE + HO. = RO2-R. + RO2. + 1.56 HCHO + 0.22 CCHO |
| | 1.68E-18 | 9.14E-15 | 5.13 | 0.00 | ETHENE + O3 = HCHO + (HCHO2) |
| | 2.18E-16 | 4.39E-13 | 4.53 | 2.00 | ETHENE + NO3 = R2O2. + RO2. + 2 HCHO + NO2 |
| | 7.42E-13 | 1.04E-11 | 1.57 | 0.00 | ETHENE + O = RO2-R. + HO2. + RO2. + HCHO + CO |
| | 2.60E-11 | 4.85E-12 | -1.00 | 0.00 | PROPENE + HO. = RO2-R. + RO2. + HCHO + CCHO |
| | 1.05E-17 | 5.51E-15 | 3.73 | 0.00 | PROPENE + O3 = 0.6 HCHO + 0.4 CCHO + 0.4 (HCHO2) + 0.6 (CCHO2) |
| | 9.74E-15 | 4.59E-13 | 2.30 | 0.00 | PROPENE + NO3 = R2O2. + RO2. + HCHO + CCHO + NO2 |
| | 4.01E-12 | 1.18E-11 | 0.64 | 0.00 | PROPENE + O = 0.4 HO2. + 0.5 RCHO + 0.5 MEK + -0.5 -C |
| | 6.30E-11 | 1.01E-11 | -1.09 | 0.00 | T-2-BUTE + HO. = RO2-R. + RO2. + 2 CCHO |
| | 1.95E-16 | 6.64E-15 | 2.10 | 0.00 | T-2-BUTE + O3 = CCHO + (CCHO2) |
| | 3.92E-13 | 1.10E-13 | -0.76 | 2.00 | T-2-BUTE + NO3 = R2O2. + RO2. + 2 CCHO + NO2 |
| | 2.34E-11 | 2.26E-11 | -0.02 | 0.00 | T-2-BUTE + O = 0.4 HO2. + 0.5 RCHO + 0.5 MEK + 0.5 -C |
| | 9.88E-11 | 2.54E-11 | -0.81 | 0.00 | ISOP + HO. = 0.088 RO2-N. + 0.912 RO2-R. + 0.629 HCHO + 0.912 ISOPROD + 0.079 R2O2. + 1.079 RO2. + 0.283 -C |
| | 1.34E-17 | 7.86E-15 | 3.80 | 0.00 | ISOP + O3 = 0.4 HCHO + 0.6 ISOPROD + 0.55 (HCHO2) + 0.2 (C:CC(C)O2) + 0.2 (C:C(C)CHO2) + 0.05 -C |
| | 3.60E-11 | (No T Dependence) | | | ISOP + O = 0.75 "ISOPROD + -C "+ 0.25 "C2CO-O2. + RCO3. + 2 HCHO + RO2-R. + RO2." |
| | 6.81E-13 | 3.03E-12 | 0.89 | 0.00 | ISOP + NO3 = 0.8 "RCHO + RNO3 + RO2-R." + 0.2 "ISOPROD + R2O2. + NO2" + RO2. + -2.2 -C |
| | 1.50E-19 | (No T Dependence) | | | ISOP + NO2 = 0.8 "RCHO + RNO3 + RO2-R." + 0.2 "ISOPROD + R2O2. + NO" + RO2. + -2.2 -C |
| | 5.31E-11 | 1.21E-11 | -0.88 | 0.00 | APIN + HO. = RO2-R. + RCHO + RO2. + 7 -C |
| | 1.00E-16 | 9.90E-16 | 1.37 | 0.00 | APIN + O3 = 0.05 HCHO + 0.2 CCHO + 0.5 RCHO + 0.61 MEK + 0.075 CO + 0.05 CCO-O2. + 0.05 C2CO-O2. + 0.1 RCO3. + 0.105 HO2. + 0.16 HO. + 0.135 RO2-R. + 0.15 R2O2. + 0.285 RO2. + 5.285 -C |
| | 6.10E-12 | 1.19E-12 | -0.97 | 0.00 | APIN + NO3 = NO2 + R2O2. + RCHO + RO2. + 7 -C |
| | 3.00E-11 | (No T Dependence) | | | APIN + O = 0.4 HO2. + 0.5 MEK + 0.5 RCHO + 6.5 -C |
| | 6.57E-11 | (No T Dependence) | | | UNKN + HO. = RO2-R. + RO2. + 0.5 HCHO + RCHO + 6.5 -C |
| | 5.85E-17 | (No T Dependence) | | | UNKN + O3 = 0.135 RO2-R. + 0.135 HO2. + 0.075 R2O2. + 0.21 RO2. + 0.025 CCO-O2. + 0.025 C2CO-O2. + 0.05 RCO3. + 0.275 HCHO + 0.175 CCHO + 0.5 RCHO + 0.41 MEK + 0.185 CO + 5.925 -C + 0.11 HO. |

Table A-2 (continued)

| Rxn. Label | Kinetic Parameters [b] k(300) | A | Ea | B | Reactions [c] |
|---|---|---|---|---|---|
| | 4.30E-12 | (No T Dependence) | | | UNKN + NO3 = R2O2. + RO2. + 0.5 HCHO + RCHO + 6.5 -C + NO2 |
| | 2.90E-11 | (No T Dependence) | | | UNKN + O = 0.4 HO2. + 0.5 RCHO + 0.5 MEK + 6.5 -C |
| | 5.91E-12 | 1.81E-12 | -0.70 | 0.00 | TOLUENE + HO. = 0.085 BALD + 0.26 CRES + 0.118 GLY + 0.847 MGLY + 0.276 AFG2 + 0.74 RO2-R. + 0.26 HO2. + 0.981 -C + 0.74 RO2. |
| | 2.36E-11 | (No T Dependence) | | | M-XYLENE + HO. = 0.04 BALD + 0.18 CRES + 0.108 GLY + 1.554 MGLY + 0.505 AFG2 + 0.82 RO2-R. + 0.18 HO2. + 0.068 -C + 0.82 RO2. |
| **Lumped Species used in EKMA Simulations** [d] | | | | | |
| A1OH | 5.11E+03 | 3.78E+03 | -0.18 | 0.00 | ALK1 + HO. = 0.911 RO2-R. + 0.074 RO2-N. + 0.005 RO2-XN. + 0.011 HO2. + 0.575 R2O2. + 1.564 RO2. + 0.065 HCHO + 0.339 CCHO + 0.196 RCHO + 0.322 ACET + 0.448 MEK + 0.024 CO + 0.025 GLY + 0.051 -C |
| A1CL | 2.00E-10 | (No T Dependence) | | | ALK1 + CL. = 0.911 RO2-R. + 0.074 RO2-N. + 0.005 RO2-XN. + 0.011 HO2. + 0.575 R2O2. + 1.564 RO2. + 0.065 HCHO + 0.339 CCHO + 0.196 RCHO + 0.322 ACET + 0.448 MEK + 0.024 CO + 0.025 GLY + 0.051 -C + HCL |
| A2OH | 1.35E+04 | 7.57E+03 | -0.35 | 0.00 | ALK2 + HO. = 0.749 RO2-R. + 0.249 RO2-N. + 0.002 RO2-XN. + 0.891 R2O2. + 1.891 RO2. + 0.029 HCHO + 0.048 CCHO + 0.288 RCHO + 0.028 ACET + 1.105 MEK + 0.043 CO + 0.018 CO2 + 1.268 -C |
| A2CL | 4.00E-10 | (No T Dependence) | | | ALK2 + CL. = 0.749 RO2-R. + 0.249 RO2-N. + 0.002 RO2-XN. + 0.891 R2O2. + 1.891 RO2. + 0.029 HCHO + 0.048 CCHO + 0.288 RCHO + 0.028 ACET + 1.105 MEK + 0.043 CO + 0.018 CO2 + 1.268 -C + HCL |
| B1OH | 8.67E+03 | (No T Dependence) | | | ARO1 + HO. = 0.742 RO2-R. + 0.258 HO2. + 0.742 RO2. + 0.015 PHEN + 0.244 CRES + 0.08 BALD + 0.124 GLY + 0.681 MGLY + 0.11 AFG1 + 0.244 AFG2 + 1.857 -C |
| B1CL | 6.00E-12 | (No T Dependence) | | | ARO1 + CL. = HCL + RO2-R. + BALD + RO2. |
| B2OH | 4.76E+04 | 1.77E+04 | -0.59 | 0.00 | ARO2 + HO. = 0.82 RO2-R. + 0.18 HO2. + 0.82 RO2. + 0.18 CRES + 0.036 BALD + 0.068 GLY + 1.02 MGLY + 0.532 AFG2 + 2.588 -C |
| B2CL | 1.20E-10 | (No T Dependence) | | | ARO2 + CL. = HCL + RO2-R. + BALD + RO2. |
| O2OH | 4.69E+04 | 3.28E+03 | -1.59 | 0.00 | OLE2 + HO. = 0.858 RO2-R. + 0.142 RO2-N. + RO2. + 0.858 HCHO + 0.252 CCHO + 0.606 RCHO + 1.267 -C |
| O2O3 | 1.59E-02 | 2.10E+00 | 2.91 | 0.00 | OLE2 + O3 = 0.6 HCHO + 0.635 RCHO + 0.981 -C + 0.4 (HCHO2) + 0.529 (CCHO2) + 0.071 (RCHO2) |
| O2N3 | 1.72E+01 | 2.94E+02 | 1.69 | 0.00 | OLE2 + NO3 = R2O2. + RO2. + HCHO + 0.294 CCHO + 0.706 RCHO + 1.451 -C + NO2 |
| O2OA | 6.07E+03 | 6.67E+03 | 0.06 | 0.00 | OLE2 + O = 0.4 HO2. + 0.5 RCHO + 0.5 MEK + 1.657 -C |
| O2CL | 2.41E-10 | (No T Dependence) | | | OLE2 + CL. = 0.4 HO2. + 0.5 RCHO + 0.5 MEK + 1.657 -C + HCL |
| O3OH | 9.21E+04 | 6.71E+03 | -1.56 | 0.00 | OLE3 + HO. = 0.861 RO2-R. + 0.139 RO2-N. + RO2. + 0.24 HCHO + 0.661 CCHO + 0.506 RCHO + 0.113 ACET + 0.086 MEK + 0.057 BALD + 0.848 -C |
| O3O3 | 2.51E-01 | 2.61E+00 | 1.40 | 0.00 | OLE3 + O3 = 0.203 HCHO + 0.358 CCHO + 0.309 RCHO + 0.061 MEK + 0.027 BALD + 0.976 -C + 0.076 (HCHO2) + 0.409 (CCHO2) + 0.279 (RCHO2) + 0.158 (C(C)CO2 + 0.039 (C(R)CO2 + 0.04 (BZCHO2) |
| O3N3 | 1.58E+03 | 4.71E+02 | -0.72 | 0.00 | OLE3 + NO3 = R2O2. + RO2. + 0.278 HCHO + 0.767 CCHO + 0.588 RCHO + 0.131 ACET + 0.1 MEK + 0.066 BALD + 0.871 -C + NO2 |
| O3OA | 3.72E+04 | 1.28E+04 | -0.64 | 0.00 | OLE3 + O = 0.4 HO2. + 0.5 RCHO + 0.5 MEK + 2.205 -C |
| O3CL | 2.70E-10 | (No T Dependence) | | | OLE6 + CL. = 0.4 HO2. + 0.5 RCHO + 0.5 MEK + 2.205 -C + HCL |

Table A-2 (continued)

| Rxn. Label | Kinetic Parameters [b] k(300) | A | Ea | B | Reactions [c] |
|---|---|---|---|---|---|
| **Reactions used to Represent Chamber-Dependent Processes** [e] | | | | | |
| O3W | (varied) | (No T Dependence) | | | O3 = |
| N25I | (varied) | (No T Dependence) | | | N2O5 = 2 NOX-WALL |
| N25S | (varied) | (No T Dependence) | | | N2O5 + H2O = 2 NOX-WALL |
| NO2W | (varied) | (No T Dependence) | | | NO2 = (yHONO) HONO + (1-yHONO) NOX-WALL |
| XSHC | (varied) | (No T Dependence) | | | HO. = HO2. |
| RSI | (Phot. File = NO2 ) | | | | HV + #RS/K1 = HO. |
| ONO2 | (Phot. File = NO2 ) | | | | HV + #E-NO2/K1 = NO2 + #-1 NOX-WALL |

[a] See Table 1 in the main body of the report for the reactions added to the general mechanism to represent chloropicrin and the Cl-containing species it forms.

[b] Except as noted, expression for rate constant is $k = A\ e^{Ea/RT}\ (T/300)^{B}$. Rate constants and A factor are in ppm, min units. Units of Ea is kcal $mole^{-1}$. For falloff kinetics the rate constants are given by $(k0[M]kINF)/(k0[M]+kINF) \times F^{X}$, where $X = 1/(1+\log_{10}(k0[M]/kINF)^{2})$. For photolysis reactions, the rate constants are calculated using the absorption cross sections in the associated "photolysis files", which are given in given in Table A-3. In addition, if "#(number)" or "#(parameter)" is given as a reactant, then the value of that number or parameter is multiplied by the result in the "rate constant expression" columns to obtain the rate constant used. Furthermore, "#RCONnn" as a reactant means that the rate constant for the reaction is obtained by multiplying the rate constant given by that for reaction "nn". Thus, the rate constant given is actually an equilibrium constant.

[c] The format of the reaction listing is the same as that used in documentation of the detailed mechanism (Carter 1990).

[d] Rate constants and product yield parameters are based on the mixture of species in the base ROG mixture which are being represented. Cl atom reactions are only applicable for reactivity simulations of chlorine-containing species, and are in addition to the reactions given on Table 1.

[e] See Table A-4 for the values of the parameters used for the specific chamber modeled in this study.

Table A-3. Absorption cross sections and quantum yields for photolysis reactions in the general mechanism.

| WL (nm) | Abs ($cm^2$) | QY | WL (nm) | Abs ($cm^2$) | QY | WL (nm) | Abs ($cm^2$) | QY | WL (nm) | Abs ($cm^2$) | QY | WL (nm) | Abs ($cm^2$) | QY |
|---|---|---|---|---|---|---|---|---|---|---|---|---|---|---|
| **Photolysis File = NO2** | | | | | | | | | | | | | | |
| 250.0 | 2.83E-20 | 1.000 | 255.0 | 1.45E-20 | 1.000 | 260.0 | 1.90E-20 | 1.000 | 265.0 | 2.05E-20 | 1.000 | 270.0 | 3.13E-20 | 1.000 |
| 275.0 | 4.02E-20 | 1.000 | 280.0 | 5.54E-20 | 1.000 | 285.0 | 6.99E-20 | 1.000 | 290.0 | 8.18E-20 | 0.999 | 295.0 | 9.67E-20 | 0.998 |
| 300.0 | 1.17E-19 | 0.997 | 305.0 | 1.66E-19 | 0.996 | 310.0 | 1.76E-19 | 0.995 | 315.0 | 2.25E-19 | 0.994 | 320.0 | 2.54E-19 | 0.993 |
| 325.0 | 2.79E-19 | 0.992 | 330.0 | 2.99E-19 | 0.991 | 335.0 | 3.45E-19 | 0.990 | 340.0 | 3.88E-19 | 0.989 | 345.0 | 4.07E-19 | 0.988 |
| 350.0 | 4.10E-19 | 0.987 | 355.0 | 5.13E-19 | 0.986 | 360.0 | 4.51E-19 | 0.984 | 365.0 | 5.78E-19 | 0.983 | 370.0 | 5.42E-19 | 0.981 |
| 375.0 | 5.35E-19 | 0.979 | 380.0 | 5.99E-19 | 0.975 | 381.0 | 5.98E-19 | 0.974 | 382.0 | 5.97E-19 | 0.973 | 383.0 | 5.96E-19 | 0.972 |
| 384.0 | 5.95E-19 | 0.971 | 385.0 | 5.94E-19 | 0.969 | 386.0 | 5.95E-19 | 0.967 | 387.0 | 5.96E-19 | 0.966 | 388.0 | 5.98E-19 | 0.964 |
| 389.0 | 5.99E-19 | 0.962 | 390.0 | 6.00E-19 | 0.960 | 391.0 | 5.98E-19 | 0.959 | 392.0 | 5.96E-19 | 0.957 | 393.0 | 5.93E-19 | 0.953 |
| 394.0 | 5.91E-19 | 0.950 | 395.0 | 5.89E-19 | 0.942 | 396.0 | 6.06E-19 | 0.922 | 397.0 | 6.24E-19 | 0.870 | 398.0 | 6.41E-19 | 0.820 |
| 399.0 | 6.59E-19 | 0.760 | 400.0 | 6.76E-19 | 0.695 | 401.0 | 6.67E-19 | 0.635 | 402.0 | 6.58E-19 | 0.560 | 403.0 | 6.50E-19 | 0.485 |
| 404.0 | 6.41E-19 | 0.425 | 405.0 | 6.32E-19 | 0.350 | 406.0 | 6.21E-19 | 0.290 | 407.0 | 6.10E-19 | 0.225 | 408.0 | 5.99E-19 | 0.185 |
| 409.0 | 5.88E-19 | 0.153 | 410.0 | 5.77E-19 | 0.130 | 411.0 | 5.88E-19 | 0.110 | 412.0 | 5.98E-19 | 0.094 | 413.0 | 6.09E-19 | 0.083 |
| 414.0 | 6.19E-19 | 0.070 | 415.0 | 6.30E-19 | 0.059 | 416.0 | 6.29E-19 | 0.048 | 417.0 | 6.27E-19 | 0.039 | 418.0 | 6.26E-19 | 0.030 |
| 419.0 | 6.24E-19 | 0.023 | 420.0 | 6.23E-19 | 0.018 | 421.0 | 6.18E-19 | 0.012 | 422.0 | 6.14E-19 | 0.008 | 423.0 | 6.09E-19 | 0.004 |
| 424.0 | 6.05E-19 | 0.000 | 425.0 | 6.00E-19 | 0.000 | | | | | | | | | |
| **Photolysis File = NO3NO** | | | | | | | | | | | | | | |
| 585.0 | 2.77E-18 | 0.000 | 590.0 | 5.14E-18 | 0.250 | 595.0 | 4.08E-18 | 0.400 | 600.0 | 2.83E-18 | 0.250 | 605.0 | 3.45E-18 | 0.200 |
| 610.0 | 1.48E-18 | 0.200 | 615.0 | 1.96E-18 | 0.100 | 620.0 | 3.58E-18 | 0.100 | 625.0 | 9.25E-18 | 0.050 | 630.0 | 5.66E-18 | 0.050 |
| 635.0 | 1.45E-18 | 0.030 | 640.0 | 1.11E-18 | 0.000 | | | | | | | | | |
| **Photolysis File = NO3NO2** | | | | | | | | | | | | | | |
| 400.0 | 0.00E+00 | 1.000 | 405.0 | 3.00E-20 | 1.000 | 410.0 | 4.00E-20 | 1.000 | 415.0 | 5.00E-20 | 1.000 | 420.0 | 8.00E-20 | 1.000 |
| 425.0 | 1.00E-19 | 1.000 | 430.0 | 1.30E-19 | 1.000 | 435.0 | 1.80E-19 | 1.000 | 440.0 | 1.90E-19 | 1.000 | 445.0 | 2.20E-19 | 1.000 |
| 450.0 | 2.80E-19 | 1.000 | 455.0 | 3.30E-19 | 1.000 | 460.0 | 3.70E-19 | 1.000 | 465.0 | 4.30E-19 | 1.000 | 470.0 | 5.10E-19 | 1.000 |
| 475.0 | 6.00E-19 | 1.000 | 480.0 | 6.40E-19 | 1.000 | 485.0 | 6.90E-19 | 1.000 | 490.0 | 8.80E-19 | 1.000 | 495.0 | 9.50E-19 | 1.000 |
| 500.0 | 1.01E-18 | 1.000 | 505.0 | 1.10E-18 | 1.000 | 510.0 | 1.32E-18 | 1.000 | 515.0 | 1.40E-18 | 1.000 | 520.0 | 1.45E-18 | 1.000 |
| 525.0 | 1.48E-18 | 1.000 | 530.0 | 1.94E-18 | 1.000 | 535.0 | 2.04E-18 | 1.000 | 540.0 | 1.81E-18 | 1.000 | 545.0 | 1.81E-18 | 1.000 |
| 550.0 | 2.36E-18 | 1.000 | 555.0 | 2.68E-18 | 1.000 | 560.0 | 3.07E-18 | 1.000 | 565.0 | 2.53E-18 | 1.000 | 570.0 | 2.54E-18 | 1.000 |
| 575.0 | 2.74E-18 | 1.000 | 580.0 | 3.05E-18 | 1.000 | 585.0 | 2.77E-18 | 1.000 | 590.0 | 5.14E-18 | 0.750 | 595.0 | 4.08E-18 | 0.600 |
| 600.0 | 2.83E-18 | 0.550 | 605.0 | 3.45E-18 | 0.400 | 610.0 | 1.45E-18 | 0.300 | 615.0 | 1.96E-18 | 0.250 | 620.0 | 3.58E-18 | 0.200 |
| 625.0 | 9.25E-18 | 0.150 | 630.0 | 5.66E-18 | 0.050 | 635.0 | 1.45E-18 | 0.000 | | | | | | |
| **Photolysis File = O3O3P** | | | | | | | | | | | | | | |
| 280.0 | 3.97E-18 | 0.100 | 281.0 | 3.60E-18 | 0.100 | 282.0 | 3.24E-18 | 0.100 | 283.0 | 3.01E-18 | 0.100 | 284.0 | 2.73E-18 | 0.100 |
| 285.0 | 2.44E-18 | 0.100 | 286.0 | 2.21E-18 | 0.100 | 287.0 | 2.01E-18 | 0.100 | 288.0 | 1.76E-18 | 0.100 | 289.0 | 1.58E-18 | 0.100 |
| 290.0 | 1.41E-18 | 0.100 | 291.0 | 1.26E-18 | 0.100 | 292.0 | 1.10E-18 | 0.100 | 293.0 | 9.89E-19 | 0.100 | 294.0 | 8.59E-19 | 0.100 |
| 295.0 | 7.70E-19 | 0.100 | 296.0 | 6.67E-19 | 0.100 | 297.0 | 5.84E-19 | 0.100 | 298.0 | 5.07E-19 | 0.100 | 299.0 | 4.52E-19 | 0.100 |
| 300.0 | 3.92E-19 | 0.100 | 301.0 | 3.42E-19 | 0.100 | 302.0 | 3.06E-19 | 0.100 | 303.0 | 2.60E-19 | 0.100 | 304.0 | 2.37E-19 | 0.100 |
| 305.0 | 2.01E-19 | 0.112 | 306.0 | 1.79E-19 | 0.149 | 307.0 | 1.56E-19 | 0.197 | 308.0 | 1.38E-19 | 0.259 | 309.0 | 1.25E-19 | 0.339 |
| 310.0 | 1.02E-19 | 0.437 | 311.0 | 9.17E-20 | 0.546 | 312.0 | 7.88E-20 | 0.652 | 313.0 | 6.77E-20 | 0.743 | 314.0 | 6.35E-20 | 0.816 |
| 315.0 | 5.10E-20 | 0.872 | 316.0 | 4.61E-20 | 0.916 | 317.0 | 4.17E-20 | 0.949 | 318.0 | 3.72E-20 | 0.976 | 319.0 | 2.69E-20 | 0.997 |
| 320.0 | 3.23E-20 | 1.000 | 330.0 | 6.70E-21 | 1.000 | 340.0 | 1.70E-21 | 1.000 | 350.0 | 4.00E-22 | 1.000 | 355.0 | 0.00E+00 | 1.000 |
| 400.0 | 0.00E+00 | 1.000 | 450.0 | 1.60E-22 | 1.000 | 500.0 | 1.34E-21 | 1.000 | 550.0 | 3.32E-21 | 1.000 | 600.0 | 5.06E-21 | 1.000 |
| 650.0 | 2.45E-21 | 1.000 | 700.0 | 8.70E-22 | 1.000 | 750.0 | 3.20E-22 | 1.000 | 800.0 | 1.60E-22 | 1.000 | 900.0 | 0.00E+00 | 1.000 |
| **Photolysis File = O3O1D** | | | | | | | | | | | | | | |
| 280.0 | 3.97E-18 | 0.900 | 281.0 | 3.60E-18 | 0.900 | 282.0 | 3.24E-18 | 0.900 | 283.0 | 3.01E-18 | 0.900 | 284.0 | 2.73E-18 | 0.900 |
| 285.0 | 2.44E-18 | 0.900 | 286.0 | 2.21E-18 | 0.900 | 287.0 | 2.01E-18 | 0.900 | 288.0 | 1.76E-18 | 0.900 | 289.0 | 1.58E-18 | 0.900 |
| 290.0 | 1.41E-18 | 0.900 | 291.0 | 1.26E-18 | 0.900 | 292.0 | 1.10E-18 | 0.900 | 293.0 | 9.89E-19 | 0.900 | 294.0 | 8.59E-19 | 0.900 |
| 295.0 | 7.70E-19 | 0.900 | 296.0 | 6.67E-19 | 0.900 | 297.0 | 5.84E-19 | 0.900 | 298.0 | 5.07E-19 | 0.900 | 299.0 | 4.52E-19 | 0.900 |
| 300.0 | 3.92E-19 | 0.900 | 301.0 | 3.42E-19 | 0.900 | 302.0 | 3.06E-19 | 0.900 | 303.0 | 2.60E-19 | 0.900 | 304.0 | 2.37E-19 | 0.900 |
| 305.0 | 2.01E-19 | 0.888 | 306.0 | 1.79E-19 | 0.851 | 307.0 | 1.56E-19 | 0.803 | 308.0 | 1.38E-19 | 0.741 | 309.0 | 1.25E-19 | 0.661 |
| 310.0 | 1.02E-19 | 0.563 | 311.0 | 9.17E-20 | 0.454 | 312.0 | 7.88E-20 | 0.348 | 313.0 | 6.77E-20 | 0.257 | 314.0 | 6.35E-20 | 0.184 |
| 315.0 | 5.10E-20 | 0.128 | 316.0 | 4.61E-20 | 0.084 | 317.0 | 4.17E-20 | 0.051 | 318.0 | 3.72E-20 | 0.024 | 319.0 | 2.69E-20 | 0.003 |
| 320.0 | 3.23E-20 | 0.000 | | | | | | | | | | | | |
| **Photolysis File = HONO** | | | | | | | | | | | | | | |
| 311.0 | 0.00E+00 | 1.000 | 312.0 | 2.00E-21 | 1.000 | 313.0 | 4.20E-21 | 1.000 | 314.0 | 4.60E-21 | 1.000 | 315.0 | 4.20E-21 | 1.000 |
| 316.0 | 3.00E-21 | 1.000 | 317.0 | 4.60E-21 | 1.000 | 318.0 | 3.60E-20 | 1.000 | 319.0 | 6.10E-20 | 1.000 | 320.0 | 2.10E-20 | 1.000 |
| 321.0 | 4.27E-20 | 1.000 | 322.0 | 4.01E-20 | 1.000 | 323.0 | 3.93E-20 | 1.000 | 324.0 | 4.01E-20 | 1.000 | 325.0 | 4.04E-20 | 1.000 |
| 326.0 | 3.13E-20 | 1.000 | 327.0 | 4.12E-20 | 1.000 | 328.0 | 7.55E-20 | 1.000 | 329.0 | 6.64E-20 | 1.000 | 330.0 | 7.29E-20 | 1.000 |
| 331.0 | 8.70E-20 | 1.000 | 332.0 | 1.38E-19 | 1.000 | 333.0 | 5.91E-20 | 1.000 | 334.0 | 5.91E-20 | 1.000 | 335.0 | 6.45E-20 | 1.000 |
| 336.0 | 5.91E-20 | 1.000 | 337.0 | 4.58E-20 | 1.000 | 338.0 | 1.91E-19 | 1.000 | 339.0 | 1.63E-19 | 1.000 | 340.0 | 1.05E-19 | 1.000 |
| 341.0 | 8.70E-20 | 1.000 | 342.0 | 3.35E-19 | 1.000 | 343.0 | 2.01E-19 | 1.000 | 344.0 | 1.02E-19 | 1.000 | 345.0 | 8.54E-20 | 1.000 |
| 346.0 | 8.32E-20 | 1.000 | 347.0 | 8.20E-20 | 1.000 | 348.0 | 7.49E-20 | 1.000 | 349.0 | 7.13E-20 | 1.000 | 350.0 | 6.83E-20 | 1.000 |
| 351.0 | 1.74E-19 | 1.000 | 352.0 | 1.14E-19 | 1.000 | 353.0 | 3.71E-19 | 1.000 | 354.0 | 4.96E-19 | 1.000 | 355.0 | 2.46E-19 | 1.000 |
| 356.0 | 1.19E-19 | 1.000 | 357.0 | 9.35E-20 | 1.000 | 358.0 | 7.78E-20 | 1.000 | 359.0 | 7.29E-20 | 1.000 | 360.0 | 6.83E-20 | 1.000 |
| 361.0 | 6.90E-20 | 1.000 | 362.0 | 7.32E-20 | 1.000 | 363.0 | 9.00E-20 | 1.000 | 364.0 | 1.21E-19 | 1.000 | 365.0 | 1.33E-19 | 1.000 |
| 366.0 | 2.13E-19 | 1.000 | 367.0 | 3.52E-19 | 1.000 | 368.0 | 4.50E-19 | 1.000 | 369.0 | 2.93E-19 | 1.000 | 370.0 | 1.19E-19 | 1.000 |
| 371.0 | 9.46E-20 | 1.000 | 372.0 | 8.85E-20 | 1.000 | 373.0 | 7.44E-20 | 1.000 | 374.0 | 4.77E-20 | 1.000 | 375.0 | 2.70E-20 | 1.000 |
| 376.0 | 1.90E-20 | 1.000 | 377.0 | 1.50E-20 | 1.000 | 378.0 | 1.90E-20 | 1.000 | 379.0 | 5.80E-20 | 1.000 | 380.0 | 7.78E-20 | 1.000 |
| 381.0 | 1.14E-19 | 1.000 | 382.0 | 1.40E-19 | 1.000 | 383.0 | 1.72E-19 | 1.000 | 384.0 | 1.99E-19 | 1.000 | 385.0 | 1.90E-19 | 1.000 |
| 386.0 | 1.19E-19 | 1.000 | 387.0 | 5.65E-20 | 1.000 | 388.0 | 3.20E-20 | 1.000 | 389.0 | 1.90E-20 | 1.000 | 390.0 | 1.20E-20 | 1.000 |
| 391.0 | 5.00E-21 | 1.000 | 392.0 | 0.00E+00 | 1.000 | | | | | | | | | |
| **Photolysis File = H2O2** | | | | | | | | | | | | | | |
| 250.0 | 8.30E-20 | 1.000 | 255.0 | 6.70E-20 | 1.000 | 260.0 | 5.20E-20 | 1.000 | 265.0 | 4.20E-20 | 1.000 | 270.0 | 3.20E-20 | 1.000 |
| 275.0 | 2.50E-20 | 1.000 | 280.0 | 2.00E-20 | 1.000 | 285.0 | 1.50E-20 | 1.000 | 290.0 | 1.13E-20 | 1.000 | 295.0 | 8.70E-21 | 1.000 |
| 300.0 | 6.60E-21 | 1.000 | 305.0 | 4.90E-21 | 1.000 | 310.0 | 3.70E-21 | 1.000 | 315.0 | 2.80E-21 | 1.000 | 320.0 | 2.00E-21 | 1.000 |
| 325.0 | 1.50E-21 | 1.000 | 330.0 | 1.20E-21 | 1.000 | 335.0 | 9.00E-22 | 1.000 | 340.0 | 7.00E-22 | 1.000 | 345.0 | 5.00E-22 | 1.000 |
| 350.0 | 3.00E-22 | 1.000 | 355.0 | 0.00E+00 | 1.000 | | | | | | | | | |

Table 3. (continued)

| WL (nm) | Abs ($cm^2$) | QY | WL (nm) | Abs ($cm^2$) | QY | WL (nm) | Abs ($cm^2$) | QY | WL (nm) | Abs ($cm^2$) | QY | WL (nm) | Abs ($cm^2$) | QY |
|---|---|---|---|---|---|---|---|---|---|---|---|---|---|---|
| **Photolysis File = CO2H** | | | | | | | | | | | | | | |
| 210.0 | 3.75E-19 | 1.000 | 220.0 | 2.20E-19 | 1.000 | 230.0 | 1.38E-19 | 1.000 | 240.0 | 8.80E-20 | 1.000 | 250.0 | 5.80E-20 | 1.000 |
| 260.0 | 3.80E-20 | 1.000 | 270.0 | 2.50E-20 | 1.000 | 280.0 | 1.50E-20 | 1.000 | 290.0 | 9.00E-21 | 1.000 | 300.0 | 5.80E-21 | 1.000 |
| 310.0 | 3.40E-21 | 1.000 | 320.0 | 1.90E-21 | 1.000 | 330.0 | 1.10E-21 | 1.000 | 340.0 | 6.00E-22 | 1.000 | 350.0 | 4.00E-22 | 1.000 |
| 360.0 | 0.00E+00 | 1.000 | | | | | | | | | | | | |
| **Photolysis File = HCHONEWR** | | | | | | | | | | | | | | |
| 280.0 | 2.49E-20 | 0.590 | 280.5 | 1.42E-20 | 0.596 | 281.0 | 1.51E-20 | 0.602 | 281.5 | 1.32E-20 | 0.608 | 282.0 | 9.73E-21 | 0.614 |
| 282.5 | 6.76E-21 | 0.620 | 283.0 | 5.82E-21 | 0.626 | 283.5 | 9.10E-21 | 0.632 | 284.0 | 3.71E-20 | 0.638 | 284.5 | 4.81E-20 | 0.644 |
| 285.0 | 3.95E-20 | 0.650 | 285.5 | 2.87E-20 | 0.656 | 286.0 | 2.24E-20 | 0.662 | 286.5 | 1.74E-20 | 0.668 | 287.0 | 1.13E-20 | 0.674 |
| 287.5 | 1.10E-20 | 0.680 | 288.0 | 2.62E-20 | 0.686 | 288.5 | 4.00E-20 | 0.692 | 289.0 | 3.55E-20 | 0.698 | 289.5 | 2.12E-20 | 0.704 |
| 290.0 | 1.07E-20 | 0.710 | 290.5 | 1.35E-20 | 0.713 | 291.0 | 1.99E-20 | 0.717 | 291.5 | 1.56E-20 | 0.721 | 292.0 | 8.65E-21 | 0.724 |
| 292.5 | 5.90E-21 | 0.727 | 293.0 | 1.11E-20 | 0.731 | 293.5 | 6.26E-20 | 0.735 | 294.0 | 7.40E-20 | 0.738 | 294.5 | 5.36E-20 | 0.741 |
| 295.0 | 4.17E-20 | 0.745 | 295.5 | 3.51E-20 | 0.749 | 296.0 | 2.70E-20 | 0.752 | 296.5 | 1.75E-20 | 0.755 | 297.0 | 1.16E-20 | 0.759 |
| 297.5 | 1.51E-20 | 0.763 | 298.0 | 3.69E-20 | 0.766 | 298.5 | 4.40E-20 | 0.769 | 299.0 | 3.44E-20 | 0.773 | 299.5 | 2.02E-20 | 0.776 |
| 300.0 | 1.06E-20 | 0.780 | 300.4 | 7.01E-21 | 0.780 | 300.6 | 8.63E-21 | 0.779 | 300.8 | 1.47E-20 | 0.779 | 301.0 | 2.01E-20 | 0.779 |
| 301.2 | 2.17E-20 | 0.779 | 301.4 | 1.96E-20 | 0.779 | 301.6 | 1.54E-20 | 0.778 | 301.8 | 1.26E-20 | 0.778 | 302.0 | 1.03E-20 | 0.778 |
| 302.2 | 8.53E-21 | 0.778 | 302.4 | 7.13E-21 | 0.778 | 302.6 | 6.61E-21 | 0.777 | 302.8 | 1.44E-20 | 0.777 | 303.0 | 3.18E-20 | 0.777 |
| 303.2 | 3.81E-20 | 0.777 | 303.4 | 5.57E-20 | 0.777 | 303.6 | 6.91E-20 | 0.776 | 303.8 | 6.58E-20 | 0.776 | 304.0 | 6.96E-20 | 0.776 |
| 304.2 | 5.79E-20 | 0.776 | 304.4 | 5.24E-20 | 0.776 | 304.6 | 4.30E-20 | 0.775 | 304.8 | 3.28E-20 | 0.775 | 305.0 | 3.60E-20 | 0.775 |
| 305.2 | 5.12E-20 | 0.775 | 305.4 | 4.77E-20 | 0.775 | 305.6 | 4.43E-20 | 0.774 | 305.8 | 4.60E-20 | 0.774 | 306.0 | 4.01E-20 | 0.774 |
| 306.2 | 3.28E-20 | 0.774 | 306.4 | 2.66E-20 | 0.774 | 306.6 | 2.42E-20 | 0.773 | 306.8 | 1.95E-20 | 0.773 | 307.0 | 1.58E-20 | 0.773 |
| 307.2 | 1.37E-20 | 0.773 | 307.4 | 1.19E-20 | 0.773 | 307.6 | 1.01E-20 | 0.772 | 307.8 | 9.01E-21 | 0.772 | 308.0 | 8.84E-21 | 0.772 |
| 308.2 | 2.08E-20 | 0.772 | 308.4 | 2.39E-20 | 0.772 | 308.6 | 3.08E-20 | 0.771 | 308.8 | 3.39E-20 | 0.771 | 309.0 | 3.18E-20 | 0.771 |
| 309.2 | 3.06E-20 | 0.771 | 309.4 | 2.84E-20 | 0.771 | 309.6 | 2.46E-20 | 0.770 | 309.8 | 1.95E-20 | 0.770 | 310.0 | 1.57E-20 | 0.770 |
| 310.2 | 1.26E-20 | 0.767 | 310.4 | 9.26E-21 | 0.764 | 310.6 | 7.71E-21 | 0.761 | 310.8 | 6.05E-21 | 0.758 | 311.0 | 5.13E-21 | 0.755 |
| 311.2 | 4.82E-21 | 0.752 | 311.4 | 4.54E-21 | 0.749 | 311.6 | 6.81E-21 | 0.746 | 311.8 | 1.04E-20 | 0.743 | 312.0 | 1.43E-20 | 0.740 |
| 312.2 | 1.47E-20 | 0.737 | 312.4 | 1.35E-20 | 0.734 | 312.6 | 1.13E-20 | 0.731 | 312.8 | 9.86E-21 | 0.728 | 313.0 | 7.82E-21 | 0.725 |
| 313.2 | 6.48E-21 | 0.722 | 313.4 | 1.07E-20 | 0.719 | 313.6 | 2.39E-20 | 0.716 | 313.8 | 3.80E-20 | 0.713 | 314.0 | 5.76E-20 | 0.710 |
| 314.2 | 6.14E-20 | 0.707 | 314.4 | 7.45E-20 | 0.704 | 314.6 | 5.78E-20 | 0.701 | 314.8 | 5.59E-20 | 0.698 | 315.0 | 4.91E-20 | 0.695 |
| 315.2 | 4.37E-20 | 0.692 | 315.4 | 3.92E-20 | 0.689 | 315.6 | 2.89E-20 | 0.686 | 315.8 | 2.82E-20 | 0.683 | 316.0 | 2.10E-20 | 0.680 |
| 316.2 | 1.66E-20 | 0.677 | 316.4 | 2.05E-20 | 0.674 | 316.6 | 4.38E-20 | 0.671 | 316.8 | 5.86E-20 | 0.668 | 317.0 | 6.28E-20 | 0.665 |
| 317.2 | 5.07E-20 | 0.662 | 317.4 | 4.33E-20 | 0.659 | 317.6 | 4.17E-20 | 0.656 | 317.8 | 3.11E-20 | 0.653 | 318.0 | 2.64E-20 | 0.650 |
| 318.2 | 2.24E-20 | 0.647 | 318.4 | 1.70E-20 | 0.644 | 318.6 | 1.24E-20 | 0.641 | 318.8 | 1.11E-20 | 0.638 | 319.0 | 7.70E-21 | 0.635 |
| 319.2 | 6.36E-21 | 0.632 | 319.4 | 5.36E-21 | 0.629 | 319.6 | 4.79E-21 | 0.626 | 319.8 | 6.48E-21 | 0.623 | 320.0 | 1.48E-20 | 0.620 |
| 320.2 | 1.47E-20 | 0.614 | 320.4 | 1.36E-20 | 0.608 | 320.6 | 1.69E-20 | 0.601 | 320.8 | 1.32E-20 | 0.595 | 321.0 | 1.49E-20 | 0.589 |
| 321.2 | 1.17E-20 | 0.583 | 321.4 | 1.15E-20 | 0.577 | 321.6 | 9.64E-21 | 0.570 | 321.8 | 7.26E-21 | 0.564 | 322.0 | 5.94E-21 | 0.558 |
| 322.2 | 4.13E-21 | 0.552 | 322.4 | 3.36E-21 | 0.546 | 322.6 | 2.39E-21 | 0.539 | 322.8 | 2.01E-21 | 0.533 | 323.0 | 1.76E-21 | 0.527 |
| 323.2 | 2.82E-21 | 0.521 | 323.4 | 4.65E-21 | 0.515 | 323.6 | 7.00E-21 | 0.508 | 323.8 | 7.80E-21 | 0.502 | 324.0 | 7.87E-21 | 0.496 |
| 324.2 | 6.59E-21 | 0.490 | 324.4 | 5.60E-21 | 0.484 | 324.6 | 4.66E-21 | 0.477 | 324.8 | 4.21E-21 | 0.471 | 325.0 | 7.77E-21 | 0.465 |
| 325.2 | 2.15E-20 | 0.459 | 325.4 | 3.75E-20 | 0.453 | 325.6 | 4.10E-20 | 0.446 | 325.8 | 6.47E-20 | 0.440 | 326.0 | 7.59E-20 | 0.434 |
| 326.2 | 6.51E-20 | 0.428 | 326.4 | 5.53E-20 | 0.422 | 326.6 | 5.76E-20 | 0.415 | 326.8 | 4.43E-20 | 0.409 | 327.0 | 3.44E-20 | 0.403 |
| 327.2 | 3.22E-20 | 0.397 | 327.4 | 2.13E-20 | 0.391 | 327.6 | 1.91E-20 | 0.384 | 327.8 | 1.42E-20 | 0.378 | 328.0 | 9.15E-21 | 0.372 |
| 328.2 | 6.79E-21 | 0.366 | 328.4 | 4.99E-21 | 0.360 | 328.6 | 4.77E-21 | 0.353 | 328.8 | 1.75E-20 | 0.347 | 329.0 | 3.27E-20 | 0.341 |
| 329.2 | 3.99E-20 | 0.335 | 329.4 | 5.13E-20 | 0.329 | 329.6 | 4.00E-20 | 0.322 | 329.8 | 3.61E-20 | 0.316 | 330.0 | 3.38E-20 | 0.310 |
| 330.2 | 3.08E-20 | 0.304 | 330.4 | 2.16E-20 | 0.298 | 330.6 | 2.09E-20 | 0.291 | 330.8 | 1.41E-20 | 0.285 | 331.0 | 9.95E-21 | 0.279 |
| 331.2 | 7.76E-21 | 0.273 | 331.4 | 6.16E-21 | 0.267 | 331.6 | 4.06E-21 | 0.260 | 331.8 | 3.03E-21 | 0.254 | 332.0 | 2.41E-21 | 0.248 |
| 332.2 | 1.74E-21 | 0.242 | 332.4 | 1.33E-21 | 0.236 | 332.6 | 2.70E-21 | 0.229 | 332.8 | 1.65E-21 | 0.223 | 333.0 | 1.17E-21 | 0.217 |
| 333.2 | 9.84E-22 | 0.211 | 333.4 | 8.52E-22 | 0.205 | 333.6 | 6.32E-22 | 0.198 | 333.8 | 5.21E-22 | 0.192 | 334.0 | 1.46E-21 | 0.186 |
| 334.2 | 1.80E-21 | 0.180 | 334.4 | 1.43E-21 | 0.174 | 334.6 | 1.03E-21 | 0.167 | 334.8 | 7.19E-22 | 0.161 | 335.0 | 4.84E-22 | 0.155 |
| 335.2 | 2.73E-22 | 0.149 | 335.4 | 1.34E-22 | 0.143 | 335.6 | -1.62E-22 | 0.136 | 335.8 | 1.25E-22 | 0.130 | 336.0 | 4.47E-22 | 0.124 |
| 336.2 | 1.23E-21 | 0.118 | 336.4 | 2.02E-21 | 0.112 | 336.6 | 3.00E-21 | 0.105 | 336.8 | 2.40E-21 | 0.099 | 337.0 | 3.07E-21 | 0.093 |
| 337.2 | 2.29E-21 | 0.087 | 337.4 | 2.46E-21 | 0.081 | 337.6 | 2.92E-21 | 0.074 | 337.8 | 8.10E-21 | 0.068 | 338.0 | 1.82E-20 | 0.062 |
| 338.2 | 3.10E-20 | 0.056 | 338.4 | 3.24E-20 | 0.050 | 338.6 | 4.79E-20 | 0.043 | 338.8 | 5.25E-20 | 0.037 | 339.0 | 5.85E-20 | 0.031 |
| 339.2 | 4.33E-20 | 0.025 | 339.4 | 4.20E-20 | 0.019 | 339.6 | 3.99E-20 | 0.012 | 339.8 | 3.11E-20 | 0.006 | 340.0 | 2.72E-20 | 0.000 |
| **Photolysis File = HCHONEWM** | | | | | | | | | | | | | | |
| 280.0 | 2.49E-20 | 0.350 | 280.5 | 1.42E-20 | 0.346 | 281.0 | 1.51E-20 | 0.341 | 281.5 | 1.32E-20 | 0.336 | 282.0 | 9.73E-21 | 0.332 |
| 282.5 | 6.76E-21 | 0.327 | 283.0 | 5.82E-21 | 0.323 | 283.5 | 9.10E-21 | 0.319 | 284.0 | 3.71E-20 | 0.314 | 284.5 | 4.81E-20 | 0.309 |
| 285.0 | 3.95E-20 | 0.305 | 285.5 | 2.87E-20 | 0.301 | 286.0 | 2.24E-20 | 0.296 | 286.5 | 1.74E-20 | 0.291 | 287.0 | 1.13E-20 | 0.287 |
| 287.5 | 1.10E-20 | 0.282 | 288.0 | 2.62E-20 | 0.278 | 288.5 | 4.00E-20 | 0.273 | 289.0 | 3.55E-20 | 0.269 | 289.5 | 2.12E-20 | 0.264 |
| 290.0 | 1.07E-20 | 0.260 | 290.5 | 1.35E-20 | 0.258 | 291.0 | 1.99E-20 | 0.256 | 291.5 | 1.56E-20 | 0.254 | 292.0 | 8.65E-21 | 0.252 |
| 292.5 | 5.90E-21 | 0.250 | 293.0 | 1.11E-20 | 0.248 | 293.5 | 6.26E-20 | 0.246 | 294.0 | 7.40E-20 | 0.244 | 294.5 | 5.36E-20 | 0.242 |
| 295.0 | 4.17E-20 | 0.240 | 295.5 | 3.51E-20 | 0.238 | 296.0 | 2.70E-20 | 0.236 | 296.5 | 1.75E-20 | 0.234 | 297.0 | 1.16E-20 | 0.232 |
| 297.5 | 1.51E-20 | 0.230 | 298.0 | 3.69E-20 | 0.228 | 298.5 | 4.40E-20 | 0.226 | 299.0 | 3.44E-20 | 0.224 | 299.5 | 2.02E-20 | 0.222 |
| 300.0 | 1.06E-20 | 0.220 | 300.4 | 7.01E-21 | 0.220 | 300.6 | 8.63E-21 | 0.221 | 300.8 | 1.47E-20 | 0.221 | 301.0 | 2.01E-20 | 0.221 |
| 301.2 | 2.17E-20 | 0.221 | 301.4 | 1.96E-20 | 0.221 | 301.6 | 1.54E-20 | 0.222 | 301.8 | 1.26E-20 | 0.222 | 302.0 | 1.03E-20 | 0.222 |
| 302.2 | 8.53E-21 | 0.222 | 302.4 | 7.13E-21 | 0.222 | 302.6 | 6.61E-21 | 0.223 | 302.8 | 1.44E-20 | 0.223 | 303.0 | 3.18E-20 | 0.223 |
| 303.2 | 3.81E-20 | 0.223 | 303.4 | 5.57E-20 | 0.223 | 303.6 | 6.91E-20 | 0.224 | 303.8 | 6.58E-20 | 0.224 | 304.0 | 6.96E-20 | 0.224 |
| 304.2 | 5.79E-20 | 0.224 | 304.4 | 5.24E-20 | 0.224 | 304.6 | 4.30E-20 | 0.225 | 304.8 | 3.28E-20 | 0.225 | 305.0 | 3.60E-20 | 0.225 |
| 305.2 | 5.12E-20 | 0.225 | 305.4 | 4.77E-20 | 0.225 | 305.6 | 4.43E-20 | 0.226 | 305.8 | 4.60E-20 | 0.226 | 306.0 | 4.01E-20 | 0.226 |
| 306.2 | 3.28E-20 | 0.226 | 306.4 | 2.66E-20 | 0.226 | 306.6 | 2.42E-20 | 0.227 | 306.8 | 1.95E-20 | 0.227 | 307.0 | 1.58E-20 | 0.227 |
| 307.2 | 1.37E-20 | 0.227 | 307.4 | 1.19E-20 | 0.227 | 307.6 | 1.01E-20 | 0.228 | 307.8 | 9.01E-21 | 0.228 | 308.0 | 8.84E-21 | 0.228 |
| 308.2 | 2.08E-20 | 0.228 | 308.4 | 2.39E-20 | 0.228 | 308.6 | 3.08E-20 | 0.229 | 308.8 | 3.39E-20 | 0.229 | 309.0 | 3.18E-20 | 0.229 |
| 309.2 | 3.06E-20 | 0.229 | 309.4 | 2.84E-20 | 0.229 | 309.6 | 2.46E-20 | 0.230 | 309.8 | 1.95E-20 | 0.230 | 310.0 | 1.57E-20 | 0.230 |
| 310.2 | 1.26E-20 | 0.233 | 310.4 | 9.26E-21 | 0.236 | 310.6 | 7.71E-21 | 0.239 | 310.8 | 6.05E-21 | 0.242 | 311.0 | 5.13E-21 | 0.245 |
| 311.2 | 4.82E-21 | 0.248 | 311.4 | 4.54E-21 | 0.251 | 311.6 | 6.81E-21 | 0.254 | 311.8 | 1.04E-20 | 0.257 | 312.0 | 1.43E-20 | 0.260 |
| 312.2 | 1.47E-20 | 0.263 | 312.4 | 1.35E-20 | 0.266 | 312.6 | 1.13E-20 | 0.269 | 312.8 | 9.86E-21 | 0.272 | 313.0 | 7.82E-21 | 0.275 |
| 313.2 | 6.48E-21 | 0.278 | 313.4 | 1.07E-20 | 0.281 | 313.6 | 2.39E-20 | 0.284 | 313.8 | 3.80E-20 | 0.287 | 314.0 | 5.76E-20 | 0.290 |
| 314.2 | 6.14E-20 | 0.293 | 314.4 | 7.45E-20 | 0.296 | 314.6 | 5.78E-20 | 0.299 | 314.8 | 5.59E-20 | 0.302 | 315.0 | 4.91E-20 | 0.305 |
| 315.2 | 4.37E-20 | 0.308 | 315.4 | 3.92E-20 | 0.311 | 315.6 | 2.89E-20 | 0.314 | 315.8 | 2.82E-20 | 0.317 | 316.0 | 2.10E-20 | 0.320 |
| 316.2 | 1.66E-20 | 0.323 | 316.4 | 2.05E-20 | 0.326 | 316.6 | 4.38E-20 | 0.329 | 316.8 | 5.86E-20 | 0.332 | 317.0 | 6.28E-20 | 0.335 |
| 317.2 | 5.07E-20 | 0.338 | 317.4 | 4.33E-20 | 0.341 | 317.6 | 4.17E-20 | 0.344 | 317.8 | 3.11E-20 | 0.347 | 318.0 | 2.64E-20 | 0.350 |
| 318.2 | 2.24E-20 | 0.353 | 318.4 | 1.70E-20 | 0.356 | 318.6 | 1.24E-20 | 0.359 | 318.8 | 1.11E-20 | 0.362 | 319.0 | 7.70E-21 | 0.365 |

Table 3. (continued)

| WL (nm) | Abs ($cm^2$) | QY | WL (nm) | Abs ($cm^2$) | QY | WL (nm) | Abs ($cm^2$) | QY | WL (nm) | Abs ($cm^2$) | QY | WL (nm) | Abs ($cm^2$) | QY |
|---|---|---|---|---|---|---|---|---|---|---|---|---|---|---|
| 319.2 | 6.36E-21 | 0.368 | 319.4 | 5.36E-21 | 0.371 | 319.6 | 4.79E-21 | 0.374 | 319.8 | 6.48E-21 | 0.377 | 320.0 | 1.48E-20 | 0.380 |
| 320.2 | 1.47E-20 | 0.386 | 320.4 | 1.36E-20 | 0.392 | 320.6 | 1.69E-20 | 0.399 | 320.8 | 1.32E-20 | 0.405 | 321.0 | 1.49E-20 | 0.411 |
| 321.2 | 1.17E-20 | 0.417 | 321.4 | 1.15E-20 | 0.423 | 321.6 | 9.64E-21 | 0.430 | 321.8 | 7.26E-21 | 0.436 | 322.0 | 5.94E-21 | 0.442 |
| 322.2 | 4.13E-21 | 0.448 | 322.4 | 3.36E-21 | 0.454 | 322.6 | 2.39E-21 | 0.461 | 322.8 | 2.01E-21 | 0.467 | 323.0 | 1.76E-21 | 0.473 |
| 323.2 | 2.82E-21 | 0.479 | 323.4 | 4.65E-21 | 0.485 | 323.6 | 7.00E-21 | 0.492 | 323.8 | 7.80E-21 | 0.498 | 324.0 | 7.87E-21 | 0.504 |
| 324.2 | 6.59E-21 | 0.510 | 324.4 | 5.60E-21 | 0.516 | 324.6 | 4.66E-21 | 0.523 | 324.8 | 4.21E-21 | 0.529 | 325.0 | 7.77E-21 | 0.535 |
| 325.2 | 2.15E-20 | 0.541 | 325.4 | 3.75E-20 | 0.547 | 325.6 | 4.10E-20 | 0.554 | 325.8 | 6.47E-20 | 0.560 | 326.0 | 7.59E-20 | 0.566 |
| 326.2 | 6.51E-20 | 0.572 | 326.4 | 5.53E-20 | 0.578 | 326.6 | 5.76E-20 | 0.585 | 326.8 | 4.43E-20 | 0.591 | 327.0 | 3.44E-20 | 0.597 |
| 327.2 | 3.22E-20 | 0.603 | 327.4 | 2.13E-20 | 0.609 | 327.6 | 1.91E-20 | 0.616 | 327.8 | 1.42E-20 | 0.622 | 328.0 | 9.15E-21 | 0.628 |
| 328.2 | 6.79E-21 | 0.634 | 328.4 | 4.99E-21 | 0.640 | 328.6 | 4.77E-21 | 0.647 | 328.8 | 1.75E-20 | 0.653 | 329.0 | 3.27E-20 | 0.659 |
| 329.2 | 3.99E-20 | 0.665 | 329.4 | 5.13E-20 | 0.671 | 329.6 | 4.00E-20 | 0.678 | 329.8 | 3.61E-20 | 0.684 | 330.0 | 3.38E-20 | 0.690 |
| 330.2 | 3.08E-20 | 0.694 | 330.4 | 2.16E-20 | 0.699 | 330.6 | 2.09E-20 | 0.703 | 330.8 | 1.41E-20 | 0.708 | 331.0 | 9.95E-21 | 0.712 |
| 331.2 | 7.76E-21 | 0.717 | 331.4 | 6.16E-21 | 0.721 | 331.6 | 4.06E-21 | 0.726 | 331.8 | 3.03E-21 | 0.730 | 332.0 | 2.41E-21 | 0.735 |
| 332.2 | 1.74E-21 | 0.739 | 332.4 | 1.33E-21 | 0.744 | 332.6 | 2.70E-21 | 0.748 | 332.8 | 1.65E-21 | 0.753 | 333.0 | 1.17E-21 | 0.757 |
| 333.2 | 9.84E-22 | 0.762 | 333.4 | 8.52E-22 | 0.766 | 333.6 | 6.32E-22 | 0.771 | 333.8 | 5.21E-22 | 0.775 | 334.0 | 1.46E-21 | 0.780 |
| 334.2 | 1.80E-21 | 0.784 | 334.4 | 1.43E-21 | 0.789 | 334.6 | 1.03E-21 | 0.793 | 334.8 | 7.19E-22 | 0.798 | 335.0 | 4.84E-22 | 0.802 |
| 335.2 | 2.73E-22 | 0.798 | 335.4 | 1.34E-22 | 0.794 | 335.6 | 0.00E+00 | 0.790 | 335.8 | 1.25E-22 | 0.786 | 336.0 | 4.47E-22 | 0.782 |
| 336.2 | 1.23E-21 | 0.778 | 336.4 | 2.02E-21 | 0.773 | 336.6 | 3.00E-21 | 0.769 | 336.8 | 2.40E-21 | 0.764 | 337.0 | 3.07E-21 | 0.759 |
| 337.2 | 2.29E-21 | 0.754 | 337.4 | 2.46E-21 | 0.749 | 337.6 | 2.92E-21 | 0.745 | 337.8 | 8.10E-21 | 0.740 | 338.0 | 1.82E-20 | 0.734 |
| 338.2 | 3.10E-20 | 0.729 | 338.4 | 3.24E-20 | 0.724 | 338.6 | 4.79E-20 | 0.719 | 338.8 | 5.25E-20 | 0.714 | 339.0 | 5.85E-20 | 0.709 |
| 339.2 | 4.33E-20 | 0.703 | 339.4 | 4.20E-20 | 0.698 | 339.6 | 3.99E-20 | 0.693 | 339.8 | 3.11E-20 | 0.687 | 340.0 | 2.72E-20 | 0.682 |
| 340.2 | 1.99E-20 | 0.676 | 340.4 | 1.76E-20 | 0.671 | 340.6 | 1.39E-20 | 0.666 | 340.8 | 1.01E-20 | 0.660 | 341.0 | 6.57E-21 | 0.655 |
| 341.2 | 4.83E-21 | 0.649 | 341.4 | 3.47E-21 | 0.643 | 341.6 | 2.23E-21 | 0.638 | 341.8 | 1.55E-21 | 0.632 | 342.0 | 3.70E-21 | 0.627 |
| 342.2 | 4.64E-21 | 0.621 | 342.4 | 1.08E-20 | 0.616 | 342.6 | 1.14E-20 | 0.610 | 342.8 | 1.79E-20 | 0.604 | 343.0 | 2.33E-20 | 0.599 |
| 343.2 | 1.72E-20 | 0.593 | 343.4 | 1.55E-20 | 0.588 | 343.6 | 1.46E-20 | 0.582 | 343.8 | 1.38E-20 | 0.576 | 344.0 | 1.00E-20 | 0.571 |
| 344.2 | 8.26E-21 | 0.565 | 344.4 | 6.32E-21 | 0.559 | 344.6 | 4.28E-21 | 0.554 | 344.8 | 3.22E-21 | 0.548 | 345.0 | 2.54E-21 | 0.542 |
| 345.2 | 1.60E-21 | 0.537 | 345.4 | 1.15E-21 | 0.531 | 345.6 | 8.90E-22 | 0.525 | 345.8 | 6.50E-22 | 0.520 | 346.0 | 5.09E-22 | 0.514 |
| 346.2 | 5.15E-22 | 0.508 | 346.4 | 3.45E-22 | 0.503 | 346.6 | 3.18E-22 | 0.497 | 346.8 | 3.56E-22 | 0.491 | 347.0 | 3.24E-22 | 0.485 |
| 347.2 | 3.34E-22 | 0.480 | 347.4 | 2.88E-22 | 0.474 | 347.6 | 2.84E-22 | 0.468 | 347.8 | 9.37E-22 | 0.463 | 348.0 | 9.70E-22 | 0.457 |
| 348.2 | 7.60E-22 | 0.451 | 348.4 | 6.24E-22 | 0.446 | 348.6 | 4.99E-22 | 0.440 | 348.8 | 4.08E-22 | 0.434 | 349.0 | 3.39E-22 | 0.428 |
| 349.2 | 1.64E-22 | 0.423 | 349.4 | 1.49E-22 | 0.417 | 349.6 | 8.30E-23 | 0.411 | 349.8 | 2.52E-23 | 0.406 | 350.0 | 2.57E-23 | 0.400 |
| 350.2 | 0.00E+00 | 0.394 | 350.4 | 5.16E-23 | 0.389 | 350.6 | 0.00E+00 | 0.383 | 350.8 | 2.16E-23 | 0.377 | 351.0 | 7.07E-23 | 0.371 |
| 351.2 | 3.45E-23 | 0.366 | 351.4 | 1.97E-22 | 0.360 | 351.6 | 4.80E-22 | 0.354 | 351.8 | 3.13E-21 | 0.349 | 352.0 | 6.41E-21 | 0.343 |
| 352.2 | 8.38E-21 | 0.337 | 352.4 | 1.55E-20 | 0.331 | 352.6 | 1.86E-20 | 0.326 | 352.8 | 1.94E-20 | 0.320 | 353.0 | 2.78E-20 | 0.314 |
| 353.2 | 1.96E-20 | 0.309 | 353.4 | 1.67E-20 | 0.303 | 353.6 | 1.75E-20 | 0.297 | 353.8 | 1.63E-20 | 0.291 | 354.0 | 1.36E-20 | 0.286 |
| 354.2 | 1.07E-20 | 0.280 | 354.4 | 9.82E-21 | 0.274 | 354.6 | 8.66E-21 | 0.269 | 354.8 | 6.44E-21 | 0.263 | 355.0 | 4.84E-21 | 0.257 |
| 355.2 | 3.49E-21 | 0.251 | 355.4 | 2.41E-21 | 0.246 | 355.6 | 1.74E-21 | 0.240 | 355.8 | 1.11E-21 | 0.234 | 356.0 | 7.37E-22 | 0.229 |
| 356.2 | 4.17E-22 | 0.223 | 356.4 | 1.95E-22 | 0.217 | 356.6 | 1.50E-22 | 0.211 | 356.8 | 8.14E-23 | 0.206 | 357.0 | 0.00E+00 | 0.200 |
| **Photolysis File = CCHOR** | | | | | | | | | | | | | | |
| 260.0 | 2.00E-20 | 0.310 | 270.0 | 3.40E-20 | 0.390 | 280.0 | 4.50E-20 | 0.580 | 290.0 | 4.90E-20 | 0.530 | 295.0 | 4.50E-20 | 0.480 |
| 300.0 | 4.30E-20 | 0.430 | 305.0 | 3.40E-20 | 0.370 | 315.0 | 2.10E-20 | 0.170 | 320.0 | 1.80E-20 | 0.100 | 325.0 | 1.10E-20 | 0.040 |
| 330.0 | 6.90E-21 | 0.000 | | | | | | | | | | | | |
| **Photolysis File = RCHO** | | | | | | | | | | | | | | |
| 280.0 | 5.26E-20 | 0.960 | 290.0 | 5.77E-20 | 0.910 | 300.0 | 5.05E-20 | 0.860 | 310.0 | 3.68E-20 | 0.600 | 320.0 | 1.66E-20 | 0.360 |
| 330.0 | 6.49E-21 | 0.200 | 340.0 | 1.44E-21 | 0.080 | 345.0 | 0.00E+00 | 0.020 | | | | | | |
| **Photolysis File = ACET-93C** | | | | | | | | | | | | | | |
| 250.0 | 2.37E-20 | 0.760 | 260.0 | 3.66E-20 | 0.800 | 270.0 | 4.63E-20 | 0.640 | 280.0 | 5.05E-20 | 0.550 | 290.0 | 4.21E-20 | 0.300 |
| 300.0 | 2.78E-20 | 0.150 | 310.0 | 1.44E-20 | 0.050 | 320.0 | 4.80E-21 | 0.026 | 330.0 | 8.00E-22 | 0.017 | 340.0 | 1.00E-22 | 0.000 |
| 350.0 | 3.00E-23 | 0.000 | 360.0 | 0.00E+00 | 0.000 | | | | | | | | | |
| **Photolysis File = KETONE** | | | | | | | | | | | | | | |
| 210.0 | 1.10E-21 | 1.000 | 220.0 | 1.20E-21 | 1.000 | 230.0 | 4.60E-21 | 1.000 | 240.0 | 1.30E-20 | 1.000 | 250.0 | 2.68E-20 | 1.000 |
| 260.0 | 4.21E-20 | 1.000 | 270.0 | 5.54E-20 | 1.000 | 280.0 | 5.92E-20 | 1.000 | 290.0 | 5.16E-20 | 1.000 | 300.0 | 3.44E-20 | 1.000 |
| 310.0 | 1.53E-20 | 1.000 | 320.0 | 4.60E-21 | 1.000 | 330.0 | 1.10E-21 | 1.000 | 340.0 | 0.00E+00 | 1.000 | | | |
| **Photolysis File = GLYOXAL1** | | | | | | | | | | | | | | |
| 230.0 | 2.87E-21 | 1.000 | 235.0 | 2.87E-21 | 1.000 | 240.0 | 4.30E-21 | 1.000 | 245.0 | 5.73E-21 | 1.000 | 250.0 | 8.60E-21 | 1.000 |
| 255.0 | 1.15E-20 | 1.000 | 260.0 | 1.43E-20 | 1.000 | 265.0 | 1.86E-20 | 1.000 | 270.0 | 2.29E-20 | 1.000 | 275.0 | 2.58E-20 | 1.000 |
| 280.0 | 2.87E-20 | 1.000 | 285.0 | 3.30E-20 | 1.000 | 290.0 | 3.15E-20 | 1.000 | 295.0 | 3.30E-20 | 1.000 | 300.0 | 3.58E-20 | 1.000 |
| 305.0 | 2.72E-20 | 1.000 | 310.0 | 2.72E-20 | 1.000 | 312.5 | 2.87E-20 | 1.000 | 315.0 | 2.29E-20 | 1.000 | 320.0 | 1.43E-20 | 1.000 |
| 325.0 | 1.15E-20 | 1.000 | 327.5 | 1.43E-20 | 1.000 | 330.0 | 1.15E-20 | 1.000 | 335.0 | 2.87E-21 | 1.000 | 340.0 | 0.00E+00 | 1.000 |
| **Photolysis File = GLYOXAL2** | | | | | | | | | | | | | | |
| 355.0 | 0.00E+00 | 1.000 | 360.0 | 2.29E-21 | 1.000 | 365.0 | 2.87E-21 | 1.000 | 370.0 | 8.03E-21 | 1.000 | 375.0 | 1.00E-20 | 1.000 |
| 380.0 | 1.72E-20 | 1.000 | 382.0 | 1.58E-20 | 1.000 | 384.0 | 1.49E-20 | 1.000 | 386.0 | 1.49E-20 | 1.000 | 388.0 | 2.87E-20 | 1.000 |
| 390.0 | 3.15E-20 | 1.000 | 391.0 | 3.24E-20 | 1.000 | 392.0 | 3.04E-20 | 1.000 | 393.0 | 2.23E-20 | 1.000 | 394.0 | 2.63E-20 | 1.000 |
| 395.0 | 3.04E-20 | 1.000 | 396.0 | 2.63E-20 | 1.000 | 397.0 | 2.43E-20 | 1.000 | 398.0 | 3.24E-20 | 1.000 | 399.0 | 3.04E-20 | 1.000 |
| 400.0 | 2.84E-20 | 1.000 | 401.0 | 3.24E-20 | 1.000 | 402.0 | 4.46E-20 | 1.000 | 403.0 | 5.27E-20 | 1.000 | 404.0 | 4.26E-20 | 1.000 |
| 405.0 | 3.04E-20 | 1.000 | 406.0 | 3.04E-20 | 1.000 | 407.0 | 2.84E-20 | 1.000 | 408.0 | 2.43E-20 | 1.000 | 409.0 | 2.84E-20 | 1.000 |
| 410.0 | 6.08E-20 | 1.000 | 411.0 | 5.07E-20 | 1.000 | 411.5 | 6.08E-20 | 1.000 | 412.0 | 4.86E-20 | 1.000 | 413.0 | 8.31E-20 | 1.000 |
| 413.5 | 6.48E-20 | 1.000 | 414.0 | 7.50E-20 | 1.000 | 414.5 | 8.11E-20 | 1.000 | 415.0 | 8.11E-20 | 1.000 | 415.5 | 6.89E-20 | 1.000 |
| 416.0 | 4.26E-20 | 1.000 | 417.0 | 4.86E-20 | 1.000 | 418.0 | 5.88E-20 | 1.000 | 419.0 | 6.69E-20 | 1.000 | 420.0 | 3.85E-20 | 1.000 |
| 421.0 | 5.67E-20 | 1.000 | 421.5 | 4.46E-20 | 1.000 | 422.0 | 5.27E-20 | 1.000 | 422.5 | 1.05E-19 | 1.000 | 423.0 | 8.51E-20 | 1.000 |
| 424.0 | 6.08E-20 | 1.000 | 425.0 | 7.29E-20 | 1.000 | 426.0 | 1.18E-19 | 1.000 | 426.5 | 1.30E-19 | 1.000 | 427.0 | 1.07E-19 | 1.000 |
| 428.0 | 1.66E-19 | 1.000 | 429.0 | 4.05E-20 | 1.000 | 430.0 | 5.07E-20 | 1.000 | 431.0 | 4.86E-20 | 1.000 | 432.0 | 4.05E-20 | 1.000 |
| 433.0 | 3.65E-20 | 1.000 | 434.0 | 4.05E-20 | 1.000 | 434.5 | 6.08E-20 | 1.000 | 435.0 | 5.07E-20 | 1.000 | 436.0 | 8.11E-20 | 1.000 |
| 436.5 | 1.13E-19 | 1.000 | 437.0 | 5.27E-20 | 1.000 | 438.0 | 1.01E-19 | 1.000 | 438.5 | 1.38E-19 | 1.000 | 439.0 | 7.70E-20 | 1.000 |
| 440.0 | 2.47E-19 | 1.000 | 441.0 | 8.11E-20 | 1.000 | 442.0 | 6.08E-20 | 1.000 | 443.0 | 7.50E-20 | 1.000 | 444.0 | 9.32E-20 | 1.000 |
| 445.0 | 1.13E-19 | 1.000 | 446.0 | 5.27E-20 | 1.000 | 447.0 | 2.43E-20 | 1.000 | 448.0 | 2.84E-20 | 1.000 | 449.0 | 3.85E-20 | 1.000 |
| 450.0 | 6.08E-20 | 1.000 | 451.0 | 1.09E-19 | 1.000 | 451.5 | 9.32E-20 | 1.000 | 452.0 | 1.22E-19 | 1.000 | 453.0 | 2.39E-19 | 1.000 |
| 454.0 | 1.70E-19 | 1.000 | 455.0 | 3.40E-19 | 1.000 | 455.5 | 4.05E-19 | 1.000 | 456.0 | 1.01E-19 | 1.000 | 457.0 | 1.62E-20 | 1.000 |

Table 3. (continued)

| WL (nm) | Abs ($cm^2$) | QY | WL (nm) | Abs ($cm^2$) | QY | WL (nm) | Abs ($cm^2$) | QY | WL (nm) | Abs ($cm^2$) | QY | WL (nm) | Abs ($cm^2$) | QY |
|---|---|---|---|---|---|---|---|---|---|---|---|---|---|---|
| 458.0 | 1.22E-20 | 1.000 | 458.5 | 1.42E-20 | 1.000 | 459.0 | 4.05E-21 | 1.000 | 460.0 | 4.05E-21 | 1.000 | 460.5 | 6.08E-21 | 1.000 |
| 461.0 | 2.03E-21 | 1.000 | 462.0 | 0.00E+00 | 1.000 | | | | | | | | | |
| **Photolysis File = MEGLYOX1** | | | | | | | | | | | | | | |
| 220.0 | 2.10E-21 | 1.000 | 225.0 | 2.10E-21 | 1.000 | 230.0 | 4.21E-21 | 1.000 | 235.0 | 7.57E-21 | 1.000 | 240.0 | 9.25E-21 | 1.000 |
| 245.0 | 8.41E-21 | 1.000 | 250.0 | 9.25E-21 | 1.000 | 255.0 | 9.25E-21 | 1.000 | 260.0 | 9.67E-21 | 1.000 | 265.0 | 1.05E-20 | 1.000 |
| 270.0 | 1.26E-20 | 1.000 | 275.0 | 1.43E-20 | 1.000 | 280.0 | 1.51E-20 | 1.000 | 285.0 | 1.43E-20 | 1.000 | 290.0 | 1.47E-20 | 1.000 |
| 295.0 | 1.18E-20 | 1.000 | 300.0 | 1.14E-20 | 1.000 | 305.0 | 9.25E-21 | 1.000 | 310.0 | 6.31E-21 | 1.000 | 315.0 | 5.47E-21 | 1.000 |
| 320.0 | 3.36E-21 | 1.000 | 325.0 | 1.68E-21 | 1.000 | 330.0 | 8.41E-22 | 1.000 | 335.0 | 0.00E+00 | 1.000 | | | |
| **Photolysis File = MEGLYOX2** | | | | | | | | | | | | | | |
| 350.0 | 0.00E+00 | 1.000 | 354.0 | 4.21E-22 | 1.000 | 358.0 | 1.26E-21 | 1.000 | 360.0 | 2.10E-21 | 1.000 | 362.0 | 2.10E-21 | 1.000 |
| 364.0 | 2.94E-21 | 1.000 | 366.0 | 3.36E-21 | 1.000 | 368.0 | 4.21E-21 | 1.000 | 370.0 | 5.47E-21 | 1.000 | 372.0 | 5.89E-21 | 1.000 |
| 374.0 | 7.57E-21 | 1.000 | 376.0 | 7.99E-21 | 1.000 | 378.0 | 8.83E-21 | 1.000 | 380.0 | 1.01E-20 | 1.000 | 382.0 | 1.09E-20 | 1.000 |
| 384.0 | 1.35E-20 | 1.000 | 386.0 | 1.51E-20 | 1.000 | 388.0 | 1.72E-20 | 1.000 | 390.0 | 2.06E-20 | 1.000 | 392.0 | 2.10E-20 | 1.000 |
| 394.0 | 2.31E-20 | 1.000 | 396.0 | 2.48E-20 | 1.000 | 398.0 | 2.61E-20 | 1.000 | 400.0 | 2.78E-20 | 1.000 | 402.0 | 2.99E-20 | 1.000 |
| 404.0 | 3.20E-20 | 1.000 | 406.0 | 3.79E-20 | 1.000 | 408.0 | 3.95E-20 | 1.000 | 410.0 | 4.33E-20 | 1.000 | 412.0 | 4.71E-20 | 1.000 |
| 414.0 | 4.79E-20 | 1.000 | 416.0 | 4.88E-20 | 1.000 | 418.0 | 5.05E-20 | 1.000 | 420.0 | 5.21E-20 | 1.000 | 422.0 | 5.30E-20 | 1.000 |
| 424.0 | 5.17E-20 | 1.000 | 426.0 | 5.30E-20 | 1.000 | 428.0 | 5.21E-20 | 1.000 | 430.0 | 5.55E-20 | 1.000 | 432.0 | 5.13E-20 | 1.000 |
| 434.0 | 5.68E-20 | 1.000 | 436.0 | 6.22E-20 | 1.000 | 438.0 | 6.06E-20 | 1.000 | 440.0 | 5.47E-20 | 1.000 | 441.0 | 6.14E-20 | 1.000 |
| 442.0 | 5.47E-20 | 1.000 | 443.0 | 5.55E-20 | 1.000 | 443.5 | 6.81E-20 | 1.000 | 444.0 | 5.97E-20 | 1.000 | 445.0 | 5.13E-20 | 1.000 |
| 446.0 | 4.88E-20 | 1.000 | 447.0 | 5.72E-20 | 1.000 | 448.0 | 5.47E-20 | 1.000 | 449.0 | 6.56E-20 | 1.000 | 450.0 | 5.05E-20 | 1.000 |
| 451.0 | 3.03E-20 | 1.000 | 452.0 | 4.29E-20 | 1.000 | 453.0 | 2.78E-20 | 1.000 | 454.0 | 2.27E-20 | 1.000 | 456.0 | 1.77E-20 | 1.000 |
| 458.0 | 8.41E-21 | 1.000 | 460.0 | 4.21E-21 | 1.000 | 464.0 | 1.68E-21 | 1.000 | 468.0 | 0.00E+00 | 1.000 | | | |
| **Photolysis File = BZCHO** | | | | | | | | | | | | | | |
| 299.0 | 1.78E-19 | 1.000 | 304.0 | 7.40E-20 | 1.000 | 306.0 | 6.91E-20 | 1.000 | 309.0 | 6.41E-20 | 1.000 | 313.0 | 6.91E-20 | 1.000 |
| 314.0 | 6.91E-20 | 1.000 | 318.0 | 6.41E-20 | 1.000 | 325.0 | 8.39E-20 | 1.000 | 332.0 | 7.65E-20 | 1.000 | 338.0 | 8.88E-20 | 1.000 |
| 342.0 | 8.88E-20 | 1.000 | 346.0 | 7.89E-20 | 1.000 | 349.0 | 7.89E-20 | 1.000 | 354.0 | 9.13E-20 | 1.000 | 355.0 | 8.14E-20 | 1.000 |
| 364.0 | 5.67E-20 | 1.000 | 368.0 | 6.66E-20 | 1.000 | 369.0 | 8.39E-20 | 1.000 | 370.0 | 8.39E-20 | 1.000 | 372.0 | 3.45E-20 | 1.000 |
| 374.0 | 3.21E-20 | 1.000 | 376.0 | 2.47E-20 | 1.000 | 377.0 | 2.47E-20 | 1.000 | 380.0 | 3.58E-20 | 1.000 | 382.0 | 9.90E-21 | 1.000 |
| 386.0 | 0.00E+00 | 1.000 | | | | | | | | | | | | |
| **Photolysis File = ACROLEIN** | | | | | | | | | | | | | | |
| 250.0 | 1.80E-21 | 1.000 | 252.0 | 2.05E-21 | 1.000 | 253.0 | 2.20E-21 | 1.000 | 254.0 | 2.32E-21 | 1.000 | 255.0 | 2.45E-21 | 1.000 |
| 256.0 | 2.56E-21 | 1.000 | 257.0 | 2.65E-21 | 1.000 | 258.0 | 2.74E-21 | 1.000 | 259.0 | 2.83E-21 | 1.000 | 260.0 | 2.98E-21 | 1.000 |
| 261.0 | 3.24E-21 | 1.000 | 262.0 | 3.47E-21 | 1.000 | 263.0 | 3.58E-21 | 1.000 | 264.0 | 3.93E-21 | 1.000 | 265.0 | 4.67E-21 | 1.000 |
| 266.0 | 5.10E-21 | 1.000 | 267.0 | 5.38E-21 | 1.000 | 268.0 | 5.73E-21 | 1.000 | 269.0 | 6.13E-21 | 1.000 | 270.0 | 6.64E-21 | 1.000 |
| 271.0 | 7.20E-21 | 1.000 | 272.0 | 7.77E-21 | 1.000 | 273.0 | 8.37E-21 | 1.000 | 274.0 | 8.94E-21 | 1.000 | 275.0 | 9.55E-21 | 1.000 |
| 276.0 | 1.04E-20 | 1.000 | 277.0 | 1.12E-20 | 1.000 | 278.0 | 1.19E-20 | 1.000 | 279.0 | 1.27E-20 | 1.000 | 280.0 | 1.27E-20 | 1.000 |
| 281.0 | 1.26E-20 | 1.000 | 282.0 | 1.26E-20 | 1.000 | 283.0 | 1.28E-20 | 1.000 | 284.0 | 1.33E-20 | 1.000 | 285.0 | 1.38E-20 | 1.000 |
| 286.0 | 1.44E-20 | 1.000 | 287.0 | 1.50E-20 | 1.000 | 288.0 | 1.57E-20 | 1.000 | 289.0 | 1.63E-20 | 1.000 | 290.0 | 1.71E-20 | 1.000 |
| 291.0 | 1.78E-20 | 1.000 | 292.0 | 1.86E-20 | 1.000 | 293.0 | 1.95E-20 | 1.000 | 294.0 | 2.05E-20 | 1.000 | 295.0 | 2.15E-20 | 1.000 |
| 296.0 | 2.26E-20 | 1.000 | 297.0 | 2.37E-20 | 1.000 | 298.0 | 2.48E-20 | 1.000 | 299.0 | 2.60E-20 | 1.000 | 300.0 | 2.73E-20 | 1.000 |
| 301.0 | 2.85E-20 | 1.000 | 302.0 | 2.99E-20 | 1.000 | 303.0 | 3.13E-20 | 1.000 | 304.0 | 3.27E-20 | 1.000 | 305.0 | 3.39E-20 | 1.000 |
| 306.0 | 3.51E-20 | 1.000 | 307.0 | 3.63E-20 | 1.000 | 308.0 | 3.77E-20 | 1.000 | 309.0 | 3.91E-20 | 1.000 | 310.0 | 4.07E-20 | 1.000 |
| 311.0 | 4.25E-20 | 1.000 | 312.0 | 4.39E-20 | 1.000 | 313.0 | 4.44E-20 | 1.000 | 314.0 | 4.50E-20 | 1.000 | 315.0 | 4.59E-20 | 1.000 |
| 316.0 | 4.75E-20 | 1.000 | 317.0 | 4.90E-20 | 1.000 | 318.0 | 5.05E-20 | 1.000 | 319.0 | 5.19E-20 | 1.000 | 320.0 | 5.31E-20 | 1.000 |
| 321.0 | 5.43E-20 | 1.000 | 322.0 | 5.52E-20 | 1.000 | 323.0 | 5.60E-20 | 1.000 | 324.0 | 5.67E-20 | 1.000 | 325.0 | 5.67E-20 | 1.000 |
| 326.0 | 5.62E-20 | 1.000 | 327.0 | 5.63E-20 | 1.000 | 328.0 | 5.71E-20 | 1.000 | 329.0 | 5.76E-20 | 1.000 | 330.0 | 5.80E-20 | 1.000 |
| 331.0 | 5.95E-20 | 1.000 | 332.0 | 6.23E-20 | 1.000 | 333.0 | 6.39E-20 | 1.000 | 334.0 | 6.38E-20 | 1.000 | 335.0 | 6.24E-20 | 1.000 |
| 336.0 | 6.01E-20 | 1.000 | 337.0 | 5.79E-20 | 1.000 | 338.0 | 5.63E-20 | 1.000 | 339.0 | 5.56E-20 | 1.000 | 340.0 | 5.52E-20 | 1.000 |
| 341.0 | 5.54E-20 | 1.000 | 342.0 | 5.53E-20 | 1.000 | 343.0 | 5.47E-20 | 1.000 | 344.0 | 5.41E-20 | 1.000 | 345.0 | 5.40E-20 | 1.000 |
| 346.0 | 5.48E-20 | 1.000 | 347.0 | 5.90E-20 | 1.000 | 348.0 | 6.08E-20 | 1.000 | 349.0 | 6.00E-20 | 1.000 | 350.0 | 5.53E-20 | 1.000 |
| 351.0 | 5.03E-20 | 1.000 | 352.0 | 4.50E-20 | 1.000 | 353.0 | 4.03E-20 | 1.000 | 354.0 | 3.75E-20 | 1.000 | 355.0 | 3.55E-20 | 1.000 |
| 356.0 | 3.45E-20 | 1.000 | 357.0 | 3.46E-20 | 1.000 | 358.0 | 3.49E-20 | 1.000 | 359.0 | 3.41E-20 | 1.000 | 360.0 | 3.23E-20 | 1.000 |
| 361.0 | 2.95E-20 | 1.000 | 362.0 | 2.81E-20 | 1.000 | 363.0 | 2.91E-20 | 1.000 | 364.0 | 3.25E-20 | 1.000 | 365.0 | 3.54E-20 | 1.000 |
| 366.0 | 3.30E-20 | 1.000 | 367.0 | 2.78E-20 | 1.000 | 368.0 | 2.15E-20 | 1.000 | 369.0 | 1.59E-20 | 1.000 | 370.0 | 1.19E-20 | 1.000 |
| 371.0 | 8.99E-21 | 1.000 | 372.0 | 7.22E-21 | 1.000 | 373.0 | 5.86E-21 | 1.000 | 374.0 | 4.69E-21 | 1.000 | 375.0 | 3.72E-21 | 1.000 |
| 376.0 | 3.57E-21 | 1.000 | 377.0 | 3.55E-21 | 1.000 | 378.0 | 2.83E-21 | 1.000 | 379.0 | 1.69E-21 | 1.000 | 380.0 | 8.29E-24 | 1.000 |
| 381.0 | 0.00E+00 | 1.000 | | | | | | | | | | | | |

Table A-4. Values for chamber wall and contaminant effects parameters used in modeling the chamber experiments for this study.

| Parm. [a] | Value(s) | Discussion |
|---|---|---|
| k(1) | 0.190 - 0.193 $min^{-1}$ | The change $NO_2$ photolysis rates over time was determined by relative $NO_2$ photolysis rates calculated from spectra taken during the experiments, with the spectrometer being held in a fixed position. These were placed on an absolute basis by separate experiments where the $NO_2$ photolysis rates were derived from measurements of low concentrations of NO, $NO_2$, and $O_3$ in steady state (Carter et al, 1995a,b). Also consistent with results of modeling $Cl_2$ - n-butane - air irradiations (unpublished results from this laboratory). |
| k(O3W) | $1.5x10^{-4}$ $min^{-1}$ | The results of the $O_3$ dark decay experiments in these chambers are consistent with the recommended default of Carter et al (1995b) for Teflon bag chambers. |
| k(N25I)<br>k(N25S) | $2.8\ x10^{-3}$ $min^{-1}$,<br>$1.5x10^{-6}$ - $k_g$ $ppm^{-1}$ $min^{-1}$ | Based on the $N_2O_5$ decay rate measurements in a similar chamber reported by Tuazon et al. (1983). Although we previously estimated there rate constants were lower in the larger Teflon bag chambers (Carter and Lurmann, 1990, 1991), we now consider it more reasonable to use the same rate constants for all such chambers (Carter et al., 1995b). |
| k(NO2W)<br>yHONO | $1.6x10^{-4}$ $min^{-1}$<br>0.2 | Based on dark $NO_2$ decay and HONO formation measured in a similar chamber by Pitts et al. (1984). Assumed to be the same in all Teflon bag chambers (Carter et al, 1995b). |
| k(XSHC) | 250 $min^{-1}$ | Estimated by modeling pure air irradiations. Not an important parameter affecting model predictions except for pure air or $NO_x$-air runs. |
| RS/K1 | $3.54x10^{6}$ $e^{-7297/T}$ ppm | Based on model simulations of n-butane - $NO_x$ experiments. The temperature dependence is derived from simulating outdoor experiments as discussed by Carter et al. (1995b). |
| E-NO2/K1 | 0.03 ppb | Based on model simulations of pure air experiments. |

[a] See Table A-2 for definition of parameters.